



12-1967

A Method for the Calculation of the Electric Microfield Distribution in a System of Charged Hard Spheres

Ronald M. Flegal
Western Michigan University

Follow this and additional works at: https://scholarworks.wmich.edu/masters_theses



Part of the Electromagnetics and Photonics Commons

Recommended Citation

Flegal, Ronald M., "A Method for the Calculation of the Electric Microfield Distribution in a System of Charged Hard Spheres" (1967). *Masters Theses*. 3235.
https://scholarworks.wmich.edu/masters_theses/3235

This Masters Thesis-Open Access is brought to you for free and open access by the Graduate College at ScholarWorks at WMU. It has been accepted for inclusion in Masters Theses by an authorized administrator of ScholarWorks at WMU. For more information, please contact wmu-scholarworks@wmich.edu.



A METHOD FOR THE CALCULATION
OF THE ELECTRIC MICROFIELD DISTRIBUTION
IN A SYSTEM OF CHARGED HARD SPHERES

by
Ronald M. Flegal

A Thesis
Submitted to the
Faculty of the School of Graduate
Studies in partial fulfillment
of the
Degree of Master of Arts

Western Michigan University
Kalamazoo, Michigan
December 1967

ACKNOWLEDGEMENTS

I wish to thank Dr. David D. Carley for providing not only the idea for this research, but also much helpful criticism and encouragement throughout the rproject. I should also like to thank Mr. Jack Meagher and the staff of the Western Michigan University Computer Center for their kind help. My special thanks goes to the staff and graduate students of the Physics Department for creating a stimulating and thoroughly enjoyable atmosphere in which it has been my pleasure to work. Finally, I should like to thank my wife, Ignacia, for her constant support while I worked on this project, and for typing the rather long and difficult manuscript that resulted from it.

Ronald M. Flegal

MASTER'S THESIS

M-1387

FLEGAL, Ronald Manley

A METHOD FOR THE CALCULATION OF THE
ELECTRIC MICROFIELD DISTRIBUTION IN A
SYSTEM OF CHARGED HARD SPHERES.

Western Michigan University, M.A., 1967
Physics, general

University Microfilms, Inc., Ann Arbor, Michigan

TABLE OF CONTENTS

CHAPTER		PAGE
I	INTRODUCTION AND HISTORICAL REVIEW	1
	1 Introduction	1
	2 The Holtsmark Distribution	2
	3 Improvements on the Holtsmark Distribution ...	5
	4 The Kelbg Theory	7
II	THE KELBG THEORY FOR A TWO COMPONENT SYSTEM	10
	5 The Two Component Model	10
	6 The Temperature-Density Parameter	17
III	EVALUATION OF THE KELBG INTEGRALS	21
	7 The Monte Carlo Method	21
	8 The Function $\exp(- \bar{X}_1 ^2 - \bar{X}_2 ^2)$	23
	9 The Function $\cos(\varphi_1 - \varphi_2)$	30
	10 The Function $\exp[- \bar{X}_1 - \bar{X}_2 ^2]$	43
IV	CONCLUSION	49
	11 Evaluation of Results	49
	12 Suggestions for Further Study	51
APPENDIX A	The Holtsmark Distribution	54
APPENDIX B	The Kelbg Theory	62
APPENDIX C	The Monte Carlo Method	68
APPENDIX D	The Simpson's Rule Calculation	76
APPENDIX E	The Monte Carlo Computer Program for the Kelbg Integrals	79
REFERENCES	84

TABLE OF FIGURES

FIGURE		PAGE
1	Monte Carlo calculation of $\langle G'(\bar{x}_1, \bar{x}_2) \rangle$, where $G'(\bar{x}_1, \bar{x}_2) = \exp[\bar{x}_1 ^2 + \bar{x}_2 ^2] G_A(\bar{x}_1, \bar{x}_2)$	28
2	The Function $G_A = g_A - 1$, for $\Theta = 4.0$, and $\sigma = 0.4$	32
3	Monte Carlo calculation of $\langle G'(\bar{x}_1, \bar{x}_2) \rangle$, where $G'(\bar{x}_1, \bar{x}_2) = \exp[\bar{x}_1 ^2 + \bar{x}_2 ^2] G_A(\bar{x}_1, \bar{x}_2) / [N - \frac{p}{N}]$	35
4	Monte Carlo calculation of $\langle G'(\bar{x}_1, \bar{x}_2) \rangle$, where $G'(\bar{x}_1, \bar{x}_2) = \exp[\bar{x}_1 ^2 + \bar{x}_2 ^2] G_A(\bar{x}_1, \bar{x}_2) / [1 + \cos(\varphi_1 - \varphi_2)]$..	42
5	Monte Carlo calculation of $\langle G'(\bar{x}_1, \bar{x}_2) \rangle$, where $G'(\bar{x}_1, \bar{x}_2) = \exp[\bar{x}_1 ^2 + \bar{x}_2 ^2 + \bar{x}_1 - \bar{x}_2 ^2] G_A(\bar{x}_1, \bar{x}_2)$	48
C.1	Block Diagram of the computer program used to make a Monte Carlo calculation.....	72
C.2	A Monte Carlo calculation of the integral $\int_{-\infty}^{+\infty} e^{- \chi } \cos \chi \, d\chi$	74
E.1	Block Diagram of the computer program used to make a Monte Carlo calculation.....	81

CHAPTER I

INTRODUCTION AND HISTORICAL REVIEW

1 Introduction

Since 1919, when work on the problem began, several theories have been developed to give the electric field distribution, $P(\bar{E})$, at a point in a completely ionized gas. (Here $P(\bar{E})$ is the probability distribution function for finding an electric field \bar{E} at the point in question. Chandrasekhar¹ shows that such a distribution can also be derived for the magnitude of the gravitational field in, say, a stellar system, since the interaction is just equal to cr^{-2} in both the electrical and gravitational cases.) The knowledge of this distribution is prerequisite to understanding the phenomenon of the broadening of spectral lines from atoms in an ionized gas,² and, using the gravitational distribution, the dynamics of stellar systems.¹ $P(\bar{E})$ may also be used to calculate $\langle E^2 \rangle = \int E^2 P(\bar{E}) d\bar{E}$, which gives the mean electric energy, U_e , of a plasma.³

The original attempt at finding $P(\bar{E})$ was made by Holtsmark, and we shall follow Chandrasekhar's treatment of the theory. In these calculations the Boltzmann factor, $U(\bar{r}_1, \dots, \bar{r}_N)/k_0 T$, was ignored, since this permits a great simplification in the theory, and gives an exact solution of the problem without further approximation. This theory is accurate, then, in the range of low density,

high temperature plasmas where particle interactions can be disregarded. However, for more dense, and/or cooler plasmas, in which the interaction between individual charged particles is significant, the Holtsmark theory is no longer valid. The problem of including interaction effects has been considered by several authors,²⁻¹³ and we shall briefly mention the more important of these later on.

In this first chapter, then, we shall give the results of the Holtsmark theory, leaving the derivation for an appendix. Later we shall outline the major attempts at improving upon Holtsmark's results, concluding with a discussion of one particular theory which we shall use as the basis for our own work.

2 The Holtsmark Distribution

A complete derivation of the Holtsmark theory is given in Appendix A of this paper, and only the essential results are presented here.

We begin by noting that Holtsmark's theory assumes a classical system of charged particles. It is further assumed that particle interactions are nonexistent, which implies that the particle distribution in space is completely random. Now the actual particle distribution in space is given by the classical Maxwell-Boltzmann equation

$$P(\bar{r}_1, \dots, \bar{r}_N) = \frac{\exp[-U(\bar{r}_1, \dots, \bar{r}_N)/k_0 T]}{\int \dots \int \exp[-U(\bar{r}_1, \dots, \bar{r}_N)/k_0 T] d\bar{r}_1 \dots d\bar{r}_N} \quad (2.1)$$

where $U(\bar{r}_1, \dots, \bar{r}_N)$ is the potential energy of the system of N particles at positions $\bar{r}_1, \dots, \bar{r}_N$ in space, k_0 is the Boltzmann constant, and T is the absolute temperature of the system.

The assumption that particle interactions can be ignored is equivalent to setting $U(\bar{r}_1, \dots, \bar{r}_N) = 0$. Thus $e^{-U/k_0 T} = 1$, and, since $\int d\bar{r}_j = V$ (the total volume of the system), we may write

$$P(\bar{r}_1, \dots, \bar{r}_N) = 1 / V^N . \quad (2.2)$$

Now the general expression for the electric field distribution can be written as

$$P(\bar{E}) = \int \dots \int P(\bar{r}_1, \dots, \bar{r}_N) \delta(\bar{E} - \sum_{i=1}^N \bar{E}_i) d\bar{r}_1 \dots d\bar{r}_N , \quad (2.3)$$

where $\delta(\bar{E} - \sum_{j=1}^N \bar{E}_j)$ is the Dirac delta function, \bar{E}_j is the electric field intensity at the field point due to a charged particle at \bar{r}_j (with respect to the field point), and \bar{E} is the total electric field intensity at the field point. Thus we may write

$$P(\bar{E}) = \frac{1}{V^N} \int \dots \int \delta(\bar{E} - \sum_{i=1}^N \bar{E}_i) d\bar{r}_1 \dots d\bar{r}_N ,$$

which is an exact expression for $P(\bar{E})$ with the assumption of no spatial correlations among the particles. This equation, however, is very difficult to solve in this form, so Holtmark turned to its Fourier transform, which is written

$$F(\bar{k}) = \iiint P(\bar{E}) \exp(i\bar{k} \cdot \bar{E}) d\bar{E} , \quad (2.4)$$

and gives, when the proper substitutions are made,

$$F(\bar{k}) = \frac{1}{V^N} \left[\iiint \exp(i\bar{k} \cdot \bar{E}) d\bar{E} \right]^N . \quad (2.5)$$

The solution to Eq.(2.5) is given in Appendix A, and we simply

note here that it is exact when N and $V \rightarrow \infty$, such that $n = N/V$ is finite and constant, and that it is written

$$F(\vec{k}) = \exp \left[-\eta \left(\frac{8\pi}{15} \right) \left(\frac{ek}{4\pi\epsilon_0} \right)^{3/2} (2\pi)^{1/2} \right], \quad (2.6)$$

where e is the charge on a singly ionized atom, and ϵ_0 is the so called permittivity of free space.

Since $P(\vec{E})$ and $F(\vec{k})$ are Fourier transform pairs we have

$$P(\vec{E}) = \frac{1}{(2\pi)^3} \iiint F(\vec{k}) \exp(-i\vec{k} \cdot \vec{E}) d\vec{k}, \quad (2.7)$$

and this equation can be solved in terms of the tabulated function

$$H(\beta) = \frac{2}{\pi\beta} \int_0^{\infty} \exp \left[-\left(\frac{x}{\beta} \right)^{3/2} \right] x \sin x dx,$$

where

$$x \equiv kE, \quad dx = E dk, \quad \beta \equiv E/A^{2/3},$$

and

$$A \equiv \left[\eta \left(\frac{8\pi}{15} \right) \left(\frac{e}{4\pi\epsilon_0} \right)^{2/3} (2\pi)^{1/2} \right].$$

Thus the final result is

$$P'(E) = 4\pi E^2 P(\vec{E}) = H(\beta) A^{-2/3}, \quad (2.8)$$

since $P(\vec{E})$ is isotropic, where $P'(E)$ is the probability distribution function for finding an electric field of magnitude $E \equiv |\vec{E}|$ at the field point.

Let us note the following characteristics of Holtmark's solution. First, it is an exact formula for $P'(E)$ (in terms of the function $H(\beta)$ which is tabulated in Appendix A) for a random distribution of charged particles in a plasma.¹ Second, the Holtmark distribution is valid only for very low particle densities ($n = N/V$ small), very high temperatures, and small field strengths, all of which are easily understood since particle

interactions are assumed to be ignorable.¹ Finally, since $U(\vec{r}_1, \dots, \vec{r}_N)$ is equal to zero in the theory, the distribution at a point is the same whether that point is electrically neutral or charged. This is because the presence of an ion or electron at the field point, or indeed at any point, can have no effect on the distribution (assumed to be completely random) of the remaining particles.

3 Improvements on the Holtsmark Distribution

Since the obvious problem with the Holtsmark distribution is that it is invalid whenever particle interactions must be considered, one would like to be able to develop a theory which would include these interactions, and, at the same time, yield the Holtsmark distribution in the high temperature, low density limit. Several attempts at such a theory have been made, as already pointed out, and in this section we shall briefly mention the two major methods of approach used.

One method for including particle interactions in the derivation of $P(\bar{E})$ follows the "collective coordinate" technique of Pines and Bohm.¹⁴ This approach was used by A.A. Broyles² and G.F. Hooper, Jr..¹⁰ Broyles' work uses the collective coordinate formalism in three ways, each of which has some shortcoming. The first two of his derivations give values for $P(\bar{E})$ which are too high and too low respectively² (for large E), and the third does not reduce to the Holtsmark distribution as $T \rightarrow \infty$ and $n \rightarrow 0$.² Hooper's Theory,¹⁰ on the other hand,

does give the Holtsmark formula for large temperature, and, although it is an extension of Broyles' work, it is valid at an ion or at a neutral point (Broyles' work is valid for an ion point only). Both theories assume an ion gas with point charges, Coulomb interactions, and a smeared-out neutralizing background. The systems are also assumed to be classical, and in thermodynamic equilibrium at temperature T . It should be noted that the collective coordinate theories are not exact, since, as is shown in the references given, they each involve several approximations.

The other major theoretical approach to the electric microfield problem is that used by Mozer^{11,12} and Kelbg.^{3,13} Both begin by expanding Eq. (2.4) in a series involving higher order correlation functions, g_n , defined by¹⁵

$$g_n(\bar{r}_1, \dots, \bar{r}_n) = \frac{V^N \int \dots \int e^{-U(\bar{r}_1, \dots, \bar{r}_n)/k_0 T} d\bar{r}_{n+1} \dots d\bar{r}_N}{\int \dots \int e^{-U(\bar{r}_1, \dots, \bar{r}_N)/k_0 T} d\bar{r}_1 \dots d\bar{r}_N} .$$

However, Mozer makes certain approximations in his expansion¹¹ which Kelbg³ does not, although both end up ignoring every term beyond the two particle correlation term ($n = 2$). Mozer, then, writes for his second correlation function, $g_2(\bar{r}_1, \bar{r}_2)$, the equation

$$g_2(\bar{r}_1, \bar{r}_2) \equiv \exp[-\phi(1,2)/k_0 T] , \quad (3.1)$$

which comes from the Debye-Huckel theory, thereby adding yet another approximation.^{11,12,16} Note that $\phi(1,2)$ is the electrostatic potential energy between particles 1 and 2, at \bar{r}_1 and \bar{r}_2 respectively.

At this point Mozer divides the field into two components, just as Broyles and Hooper do. The electron cloud being treated like a system of point charges with Coulomb interactions and a uniform, smeared-out, neutralizing background of ions, while the ions are not treated with Coulomb interactions, but are assumed to be shielded by an electron cloud with one electron for each ion. The Debye-Huckel theory is again employed to derive the shielding while the ion-ion interactions are neglected. Mozer's results like Hooper's and Broyles' are given separately for the electron and ion fields, and, like Hooper's, for neutral points and charged (ion) points, as well as for various values of the temperature and particle density.

This concludes, with one exception, our description of some of the approaches to the solution of the microfield problem. So far only the Holtsmark theory has been presented with any completeness, since it is the limiting case of all results. The other methods were mentioned here only to acquaint the reader in a general way with what has been done to include particle interactions.

4 The Kelbg Theory

As before we shall leave the formal development of the theory for an appendix, and present here only the essential results.

Kelbg^{3,13} begins with Eqs.(2.3)-(2.4), but does not allow $U(\vec{r}_1, \dots, \vec{r}_N)$ to go to zero. Hence, as is shown in Appendix B,

Eq. (2.4) becomes

$$F(\bar{k}) = \prod_{j=1}^N \omega_j \left[1 + \frac{1}{2V^2} \sum_{i < j} \iint \left(\frac{\Omega_i \Omega_j}{\omega_i \omega_j} - 1 \right) g_{ij} d\bar{r}_i d\bar{r}_j + \dots \right], \quad (4.1)$$

where $\Omega_i \equiv \exp[i\bar{k} \cdot \bar{E}_i]$ and $\omega_i = \frac{1}{V} \int \Omega_i g_i d\bar{r}_i$.

Notice that $V \equiv$ Volume of the system, $N \equiv$ the number of particles in the system, $g_{ij} \equiv g_2(\bar{r}_i, \bar{r}_j)$ and $g_j = g_1(\bar{r}_j)$, as defined in section 3 of this paper.¹⁵

At this point Kelbg shows (see Appendix B) that the term $\prod_{j=1}^N \omega_j$ is just the Holtmark expression and he writes it in the form

$$F_0(\bar{k}) \equiv \exp \left[\sum_{\sigma=1}^s n_{\sigma} \int (\Omega_{\sigma} - 1) g_{\sigma}(\bar{r}_{\sigma}) d\bar{r}_{\sigma} \right], \quad (4.2)$$

leaving

$$F_1(\bar{k}) \equiv \left[1 + \frac{1}{2V^2} \iint \sum_{i < j} \left(\frac{\Omega_i \Omega_j}{\omega_i \omega_j} - 1 \right) g_2(\bar{r}_i, \bar{r}_j) d\bar{r}_i d\bar{r}_j + \dots \right]. \quad (4.3)$$

Now, in Eq. (4.2), σ labels the different types of particles, and n_{σ} their number densities. Thus for a two component system,

$$\sum_{\sigma=1}^s \text{ becomes } \sum_{\sigma=1}^2,$$

and if there are the same number of particles of each type, then

$n_1 = n_2$. Note also that in order to write $\prod_{j=1}^N \omega_j$ in the form of Eq. (4.2) it is assumed that N_{σ} (the number of particles of each type) approaches infinity along with V , leaving $n_{\sigma} = N_{\sigma}/V$ constant and finite. Thus, since the Holtmark term is already tabulated, only $F_1(\bar{k})$ is left to be found before $F(\bar{k})$ can be completely known. Of course, once this is known, for values of k from zero to infinity, one is in a position to find $P(\bar{E})$,

using the equation

$$P(\bar{E}) = \frac{1}{(2\pi)^3} \iiint F(\bar{k}) \exp(-i\bar{k}\cdot\bar{E}) d\bar{k}. \quad (4.4)$$

It is, then, at this point that Kelbg makes his only approximation.³ He writes Eq.(4.3) in the form —

$$F_1(\bar{k}) = \exp\left[\frac{1}{2} \sum_{\sigma=1}^s \sum_{\tau=1}^s n_{\sigma} n_{\tau} \iint \left(\frac{\Omega_{\sigma} \Omega_{\tau}}{\omega_{\sigma} \omega_{\tau}} - 1\right) g_2 d\bar{r}_{\sigma} d\bar{r}_{\tau}\right], \quad (4.5)$$

thereby assuming that all terms of higher order than the two particle interaction term are small. This makes physical sense for low densities where the chance of interactions involving three and more particles is small. For higher densities, however, the higher order terms would presumably contribute substantially, although these terms would be very difficult to calculate. Thus since this theory does consider two body correlations it should be valid for higher densities than the Holtsmark theory, but there will still be a limiting density above which Kelbg's equations too are valid.

In summary, then, we have given an introduction to the problem of finding $P(\bar{E})$, the electric microfield distribution, having mentioned some approaches to its solution. We have concluded with the Kelbg theory, and have stated that if Eq.(4.5) can be solved for all values of k , then $P(\bar{E})$ can be found. In the next chapter we shall put this equation in a form which is "soluble" via numerical methods, and, at the same time, introduce the temperature and the density parameters upon which its solution will depend.

CHAPTER II

THE KELBG THEORY FOR A TWO COMPONENT SYSTEM

5 The Two Component Model

The purpose of this thesis is to bring together the electric microfield theory of Kelbg, and the recently calculated two component radial distribution functions of D.D. Carley,¹⁷ in a new theory for the calculation of $P(\bar{E})$. In particular we shall find a way of evaluating Eq.(4.5) for all values of k for a particular physical system.

The system, or model, we choose must be identical to that used by Carley in calculating g_2 . It is not, however, our purpose to evaluate or interpret g_2 , although the interested reader may refer to T.L. Hill,¹⁵ in addition to Carley's paper, to get this information. For our work g_2 is simply a tabulated, two particle correlation function which must be plugged into Eq.(4.5) to give $F_1(\bar{k})$, and we choose to use these particular g_2 functions. Note that the techniques for evaluating Eq.(4.5) will not depend on what g 's are used. Hence we are not limited to the model given here, and if a better method for calculating g is found, its results may easily be used with our equations. Our model then is a classical system of N hard spheres, half of which are positively charged and half negatively charged. These spheres are assumed to be enclosed in a volume V , in thermodynamic

equilibrium at temperature T . The number density of the positive and negative particles is given by $n = N/2V$, and is assumed to remain constant as N and V go to infinity.

Applying this model to Eq.(4.2), and referring to Appendix A, we have

$$\begin{aligned} F_0(\bar{k}) &= \exp \left\{ n_A \int (e^{i\bar{k} \cdot \bar{E}_A} - 1) g_1(\bar{r}_A) d\bar{r}_A + n_B \int (e^{i\bar{k} \cdot \bar{E}_B} - 1) g_2(\bar{r}_B) d\bar{r}_B \right\} \\ &= \exp \left\{ -n \int (1 - e^{i\bar{k} \cdot \bar{E}_A}) g_1(\bar{r}_A) d\bar{r}_A \right\} \exp \left\{ -n \int (1 - e^{i\bar{k} \cdot \bar{E}_B}) g_2(\bar{r}_B) d\bar{r}_B \right\} \\ &= \exp \left\{ -2n \int (1 - e^{i\bar{k} \cdot \bar{E}_A}) g_1(\bar{r}_A) d\bar{r}_A \right\}. \end{aligned}$$

This equation results because $\bar{E}_A = -\bar{E}_B$, enabling us to write everything in terms of \bar{E}_A , as indicated at the end of Appendix A.

Note also that the functional form of $g_1(\bar{r}_A)$ is the same as $g_1(\bar{r}_B)$.

Thus for the model used here

$$F_0(\bar{k}) = \exp \left\{ -2n \left(\frac{8\pi}{15} \right) (kc)^{3/2} (2\pi)^{1/2} \right\} \quad (5.1)$$

where $n = N/2V$, $k = \bar{k}$, and $c = \frac{+e}{4\pi \epsilon_0}$. Clearly $F_0(\bar{k})$ depends on the number density for a given k , with the singly charged particles assumed here, and different values of n may be used depending on the physical system.

Turning now to Eq.(4.5) we write the two component correction term as

$$F_1(\bar{k}) = \exp \left\{ \frac{1}{2} \sum_{\sigma=A}^B \sum_{\tau=A}^B n_\sigma n_\tau \iint \left(\frac{\Omega_\sigma \Omega_\tau}{\omega_\sigma \omega_\tau} - 1 \right) g_2(\bar{r}_\sigma, \bar{r}_\tau) d\bar{r}_\sigma d\bar{r}_\tau \right\}.$$

Now $n_\sigma = n_\tau = N/2V$ as we have already stated. Also note that

$$\begin{aligned}
\omega_{\sigma} &\equiv \int \exp(i \bar{k} \cdot \bar{E}_{\sigma}) P_1(\bar{r}_{\sigma}) d\bar{r}_{\sigma} \\
&= \int \exp(i \bar{k} \cdot \bar{E}_{\sigma}) \frac{g_1(\bar{r}_{\sigma})}{V} d\bar{r}_{\sigma} \\
&= \frac{1}{V} \int \exp(i \bar{k} \cdot \bar{E}_{\sigma}) d\bar{r}_{\sigma},
\end{aligned}$$

since $g_1(\bar{r}_{\sigma}) = 1$ at a neutral point. Hence

$$\begin{aligned}
\omega_{\sigma} &= \frac{1}{V} \int (e^{i \bar{k} \cdot \bar{E}_{\sigma}} - 1 + 1) d\bar{r}_{\sigma} \\
&= \frac{1}{V} \left[\int d\bar{r}_{\sigma} - \int (1 - e^{i \bar{k} \cdot \bar{E}_{\sigma}}) d\bar{r}_{\sigma} \right] \\
&= \frac{1}{V} \left[V - \frac{8}{15} (2\pi)(kC)^{3/2} \left(\frac{\pi}{2}\right)^{1/2} \right] \\
&= 1 - \frac{1}{V} \left[\left(\frac{8\pi}{15}\right) (2\pi)^{1/2} (kC)^{3/2} \right].
\end{aligned}$$

This comes from Eq.(A.9) in Appendix A, and, since we are assuming that N and V go to infinity, then $\omega_{\sigma} = 1$ for neutral point calculations. Thus we can write

$$\begin{aligned}
F_1(\bar{k}) &= \exp \left[\frac{1}{2} n^2 \left\{ \iint (\Omega_{A1} \Omega_{A2} - 1) g_2(\bar{r}_{A1}, \bar{r}_{A2}) d\bar{r}_{A1} d\bar{r}_{A2} \right. \right. \\
&\quad + \iint (\Omega_{A1} \Omega_{B2} - 1) g_2(\bar{r}_{A1}, \bar{r}_{B2}) d\bar{r}_{A1} d\bar{r}_{B2} \\
&\quad + \iint (\Omega_{B1} \Omega_{A2} - 1) g_2(\bar{r}_{B1}, \bar{r}_{A2}) d\bar{r}_{B1} d\bar{r}_{A2} \\
&\quad \left. \left. + \iint (\Omega_{B1} \Omega_{B2} - 1) g_2(\bar{r}_{B1}, \bar{r}_{B2}) d\bar{r}_{B1} d\bar{r}_{B2} \right\} \right], \quad (5.2)
\end{aligned}$$

where the A subscripts refer to positively charged particles,

and the B subscripts to negatively charged particles. The 1 and 2 subscripts refer to the particular particles in the integrals. Hence \vec{r}_1 is the position vector of particle one, while $\Omega_{A1} = e^{i\vec{k} \cdot \vec{E}_{A1}}$ indicates that particle one is a positively charged particle, since

$$\vec{E}_{A1} \equiv \frac{e}{4\pi\epsilon_0} \frac{\vec{r}_1}{r_1^3}.$$

Now

$$\Omega_{A1} \Omega_{B2} = \exp \left\{ i\vec{k} \cdot \left(\frac{e\vec{r}_1}{4\pi\epsilon_0 r_1^3} - \frac{e\vec{r}_2}{4\pi\epsilon_0 r_2^3} \right) \right\},$$

but this has the same functional form as

$$\Omega_{B1} \Omega_{A2} = \exp \left\{ i\vec{k} \cdot \left(\frac{e\vec{r}_2}{4\pi\epsilon_0 r_2^3} - \frac{e\vec{r}_1}{4\pi\epsilon_0 r_1^3} \right) \right\},$$

except for a minus sign. Note also that $g_2(\vec{r}_{A1}, \vec{r}_{B2}) = g_2(\vec{r}_{B1}, \vec{r}_{A2})$, from the definition of g_n given on page 6 of this paper. Hence the second and third integrals in the exponent in Eq.(5.2) are identical if we just switch the particle indexes (1 and 2 subscripts) in one of them. This we can do since the switch does not effect the functional form of the integrand, and the two integrals can thereby be combined into one. The same argument may also be applied to the first and fourth integrals in Eq.(5.2) resulting in the much more compact expression

$$F_1(\vec{k}) = \exp \left\{ \frac{1}{2} n^2 \left[\iint (\Omega_{A1} \Omega_{A2} + \Omega_{B1} \Omega_{B2} - 2) g_2(\vec{r}_{A1}, \vec{r}_{A2}) d\vec{r}_1 d\vec{r}_2 \right. \right. \\ \left. \left. + \iint (\Omega_{A1} \Omega_{B2} + \Omega_{B1} \Omega_{A2} - 2) g_2(\vec{r}_{A1}, \vec{r}_{B2}) d\vec{r}_1 d\vec{r}_2 \right] \right\}. \quad (5.3)$$

Note that $g_{AA}(\vec{r}_1, \vec{r}_2) \neq g_{AB}(\vec{r}_1, \vec{r}_2)$, since the distribution of like charges about each other is not equal to that of unlike charges, and that $g_2(\vec{r}_{A1}, \vec{r}_{A2}) = g_2(\vec{r}_{B1}, \vec{r}_{B2})$ for this model,

although the latter is not true in general.¹⁷

At this point we shall make a substitution which will make it more convenient to evaluate Eq.(5.3) numerically. Let $g_2(\bar{r}_{A1}, \bar{r}_{A2})$ be equal to $G_A(\bar{r}_1, \bar{r}_2) + 1$, and $g_2(\bar{r}_{A1}, \bar{r}_{B2}) = G_B(\bar{r}_1, \bar{r}_2) + 1$. Thus our equation takes the form

$$\begin{aligned}
 & \iint \left(\frac{\Omega_1 \Omega_2}{\omega_1 \omega_2} - 1 \right) (G(\bar{r}_1, \bar{r}_2) + 1) d\bar{r}_1 d\bar{r}_2 \\
 = & \iint \frac{\Omega_1 \Omega_2}{\omega_1 \omega_2} G(\bar{r}_1, \bar{r}_2) d\bar{r}_1 d\bar{r}_2 + \iint \frac{\Omega_1 \Omega_2}{\omega_1 \omega_2} d\bar{r}_1 d\bar{r}_2 \\
 & - \iint G(\bar{r}_1, \bar{r}_2) d\bar{r}_1 d\bar{r}_2 - \iint d\bar{r}_1 d\bar{r}_2 \\
 = & \iint \left(\frac{\Omega_1 \Omega_2}{\omega_1 \omega_2} - 1 \right) G(\bar{r}_1, \bar{r}_2) d\bar{r}_1 d\bar{r}_2 + V^2 \frac{\iint \Omega_1 \Omega_2 d\bar{r}_1 d\bar{r}_2}{\iint \Omega_1 \Omega_2 d\bar{r}_1 d\bar{r}_2} - V^2 \\
 = & \iint \left(\frac{\Omega_1 \Omega_2}{\omega_1 \omega_2} - 1 \right) G(\bar{r}_1, \bar{r}_2) d\bar{r}_1 d\bar{r}_2 , \tag{5.4}
 \end{aligned}$$

where $\omega_i = \frac{1}{V} \int \Omega_i d\bar{r}_i$, and $G(\bar{r}_1, \bar{r}_2) = g_2(\bar{r}_1, \bar{r}_2) - 1$ for either the "AA" or the "AB" case in Eq.(5.3). Note that this is just an identity, and we shall use the functions $G(\bar{r}_1, \bar{r}_2)$ in our numerical calculations later on.

One final change will be made in Eq.(5.3), and again we shall use only algebraic and trigonometric identities. Hence we write

$$\begin{aligned}
 \Omega_{A1} \Omega_{A2} &= \exp \left[i \bar{k} \cdot (\bar{E}_{A1} + \bar{E}_{A2}) \right] \\
 &\equiv \cos \left[\bar{k} \cdot (\bar{E}_{A1} + \bar{E}_{A2}) \right] + i \sin \left[\bar{k} \cdot (\bar{E}_{A1} + \bar{E}_{A2}) \right],
 \end{aligned}$$

by Euler's Theorem. But

$$\cos(A \pm B) = \cos A \cos B \mp \sin A \sin B,$$

and

$$\sin(A \pm B) = \sin A \cos B \pm \cos A \sin B,$$

by trigonometric identity. Note also that

$$\cos(\pm A) = \cos A,$$

while

$$\sin(\pm A) = \pm \sin A.$$

And finally note that $\bar{E}_{A1} = -\bar{E}_{B1}$, i.e. if particle one is negative, its electric field vector \bar{E}_{B1} can be replaced by $-\bar{E}_{A1}$ without changing anything. Putting this all together, then, gives us

$$\begin{aligned} \Omega_{A1} \Omega_{A2} &= \cos(\bar{k} \cdot \bar{E}_{A1}) \cos(\bar{k} \cdot \bar{E}_{A2}) - \sin(\bar{k} \cdot \bar{E}_{A1}) \sin(\bar{k} \cdot \bar{E}_{A2}) \\ &\quad + i \sin(\bar{k} \cdot \bar{E}_{A1}) \cos(\bar{k} \cdot \bar{E}_{A2}) + i \sin(\bar{k} \cdot \bar{E}_{A2}) \cos(\bar{k} \cdot \bar{E}_{A1}), \end{aligned}$$

so

$$\begin{aligned} \Omega_{B1} \Omega_{B2} + \Omega_{A1} \Omega_{A2} &= 2 \left[\cos(\bar{k} \cdot \bar{E}_{A1}) \cos(\bar{k} \cdot \bar{E}_{A2}) \right. \\ &\quad \left. - \sin(\bar{k} \cdot \bar{E}_{A1}) \sin(\bar{k} \cdot \bar{E}_{A2}) \right] \\ &\quad + i \left[\sin(\bar{k} \cdot \bar{E}_{A1}) \cos(\bar{k} \cdot \bar{E}_{A2}) + \sin(\bar{k} \cdot \bar{E}_{A2}) \cos(\bar{k} \cdot \bar{E}_{A1}) \right. \\ &\quad \left. - \sin(\bar{k} \cdot \bar{E}_{A1}) \cos(\bar{k} \cdot \bar{E}_{A2}) - \sin(\bar{k} \cdot \bar{E}_{A2}) \cos(\bar{k} \cdot \bar{E}_{A1}) \right] \\ &= 2 \cos \left[\bar{k} \cdot (\bar{E}_{A1} + \bar{E}_{A2}) \right], \end{aligned} \tag{5.4}$$

and

$$\begin{aligned}
\Omega_{A1}\Omega_{B2} + \Omega_{B1}\Omega_{A2} &= \exp[i\vec{k}\cdot(\vec{E}_{A1}-\vec{E}_{A2})] + \exp[i\vec{k}\cdot(\vec{E}_{A2}-\vec{E}_{A1})] \\
&= \cos(\vec{k}\cdot\vec{E}_{A1})\cos(\vec{k}\cdot\vec{E}_{A2}) + \sin(\vec{k}\cdot\vec{E}_{A1})\sin(\vec{k}\cdot\vec{E}_{A2}) \\
&\quad + \cos(\vec{k}\cdot\vec{E}_{A2})\cos(\vec{k}\cdot\vec{E}_{A1}) + \sin(\vec{k}\cdot\vec{E}_{A2})\sin(\vec{k}\cdot\vec{E}_{A1}) \\
&\quad + i\sin(\vec{k}\cdot\vec{E}_{A1})\cos(\vec{k}\cdot\vec{E}_{A2}) - i\cos(\vec{k}\cdot\vec{E}_{A1})\sin(\vec{k}\cdot\vec{E}_{A2}) \\
&\quad + i\sin(\vec{k}\cdot\vec{E}_{A2})\cos(\vec{k}\cdot\vec{E}_{A1}) - i\cos(\vec{k}\cdot\vec{E}_{A2})\sin(\vec{k}\cdot\vec{E}_{A1}) \\
&= 2 \cos[\vec{k}\cdot(\vec{E}_{A1}-\vec{E}_{A2})] . \tag{5.5}
\end{aligned}$$

Clearly, then, upon substitution of Eqs.(5.4) and (5.5) into Eq.(5.3) we get

$$\begin{aligned}
F_1(\vec{k}) &= \exp\left[\eta^2 \left\{ \iint (\cos[\vec{k}\cdot(\vec{E}_{A1}+\vec{E}_{A2})] - 1) G_A(\vec{r}_1, \vec{r}_2) d\vec{r}_1 d\vec{r}_2 \right. \right. \\
&\quad \left. \left. + \iint (\cos[\vec{k}\cdot(\vec{E}_{A1}-\vec{E}_{A2})] - 1) G_B(\vec{r}_1, \vec{r}_2) d\vec{r}_1 d\vec{r}_2 \right\} \right], \tag{5.6}
\end{aligned}$$

which is the form of the two component correction term that we shall work with.

Upon combining Eq.(5.1) and Eq.(5.6) we can finally write down $F(\vec{k})$ in a form which reflects our two component model, and is easy to work with. Thus,

$$\begin{aligned}
F(\vec{k}) &= F_0(\vec{k}) F_1(\vec{k}) \\
&= \exp\left[-2\eta \left(\frac{8\pi}{15}\right) (kc)^{3/2} (2\pi)^{1/2}\right] \\
&\quad \times \exp\left[\eta^2 \left\{ \iint (\cos[\vec{k}\cdot(\vec{E}_{A1}+\vec{E}_{A2})] - 1) G_A(\vec{r}_1, \vec{r}_2) d\vec{r}_1 d\vec{r}_2 \right. \right. \\
&\quad \left. \left. + \iint (\cos[\vec{k}\cdot(\vec{E}_{A1}-\vec{E}_{A2})] - 1) G_B(\vec{r}_1, \vec{r}_2) d\vec{r}_1 d\vec{r}_2 \right\} \right],
\end{aligned}$$

where

$$\eta \equiv N / 2V ,$$

$$C \equiv \frac{e}{4\pi\epsilon_0} ,$$

$$E_{Ai} = C \bar{r}_i / r_i^3 ,$$

$$G_{AB}(\bar{r}_1, \bar{r}_2) = g_{AB}(\bar{r}_1, \bar{r}_2) - 1 ,$$

$N \equiv$ total number of particles in the system,

$V \equiv$ total volume of the system,

and $e \equiv$ the charge on the positively charged particles.

6 The Temperature-Density Parameter

As was shown in the last section $F_o(\bar{k})$ depends on n for a given k (e is assumed to equal the positive electronic charge, throughout this paper.). It is also easy to see that $F_1(\bar{k})$ depends on n for a given k , if $G(\bar{r}_1, \bar{r}_2)$ depends on n . Carley¹⁷ shows, in fact, that $G(\bar{r}_1, \bar{r}_2)$ depends on two parameters, σ , and θ . Here σ is the particle diameter, and

$$\theta \equiv \frac{k_o T a}{e^2} , \quad (6.1)$$

where k_o is the Boltzmann constant, T is the absolute temperature, and a is a unit of length. We define this unit by

$$a \equiv \left[\frac{3}{4\pi\eta} \right]^{1/3} , \quad (6.2)$$

so it is equal to the radius of a sphere, in our system, which contains, on the average, one positive particle. Hence $G(\bar{r}_1, \bar{r}_2)$

is a function of n and/or T (a given Θ defining a whole range of coupled n and T values), and is equal to zero if $|\bar{r}_1 - \bar{r}_2| < \sigma$, corresponding to our requirement that the particles be hard spheres of radius $\sigma/2$.

It is clear, then, that $F(\bar{k})$ depends not only on the variable k , but also upon a certain temperature-density parameter Θ .

Thus we wish to include Θ in our equations, and to do so we write

$$\Theta \equiv \frac{k_0 T a}{e^2},$$

$$a \equiv \left[\frac{3}{4\pi n} \right]^{1/3},$$

and

$$\bar{\mathcal{E}} \equiv \frac{e a}{k_0 T} \bar{E}. \quad (6.3)$$

Now Eq. (6.3) simply defines a new electric field vector as a constant multiple of the old one, so $\bar{\mathcal{E}}$ may be inserted in our equations, in place of \bar{E} , from the beginning without changing anything. Let us also define

$$\chi \equiv \frac{r}{a}$$

to be a length in units of a . We may now write

$$\begin{aligned} \bar{\mathcal{E}} &\equiv \frac{e a}{k_0 T} \bar{E} \\ &= \frac{e a}{k_0 T} \bar{E} \quad (\text{in Gaussian units}) \\ &= \frac{e^2 a}{k_0 T} \frac{\bar{\chi} a}{|\bar{\chi}|^3 a^3} \\ &= \bar{\chi} / |\bar{\chi}|^3 \Theta. \end{aligned} \quad (6.4)$$

Using $\bar{\mathcal{E}}$ instead of \bar{E} , we have $c = (e^2 a^2)/(k_0 T a)$, giving

$$\begin{aligned}
F_0(\bar{k}) &= \exp\left[-2\eta\left(\frac{8\pi}{15}\right) (c k)^{3/2} (2\pi)^{1/2}\right] \\
&= \exp\left[-\frac{6}{4\pi a^3} \left(\frac{8\pi}{15}\right) \left(\frac{e^2 a^4}{k_0 T a}\right) k^{3/2} (2\pi)^{1/2}\right] \\
&= \exp\left[-\frac{4}{5} \left(\frac{k}{\Theta}\right)^{3/2} (2\pi)^{1/2}\right], \tag{6.5}
\end{aligned}$$

and

$$\begin{aligned}
F_1(\bar{k}) &= \exp\left[\frac{9}{16\pi^2 a^6} \left\{ \iint (\cos\left[\frac{\bar{k}}{\Theta} \cdot \left(\frac{\bar{X}_1}{|\bar{X}_1|^3} + \frac{\bar{X}_2}{|\bar{X}_2|^3}\right)\right] - 1\right) G_A a^6 d\bar{X}_1 d\bar{X}_2 \right. \right. \\
&\quad \left. \left. + \iint (\cos\left[\frac{\bar{k}}{\Theta} \cdot \left(\frac{\bar{X}_1}{|\bar{X}_1|^3} - \frac{\bar{X}_2}{|\bar{X}_2|^3}\right)\right] - 1\right) G_B a^6 d\bar{X}_1 d\bar{X}_2 \right\} \right] \\
&= \exp\left[\left(\frac{3}{4\pi}\right)^2 \left\{ \iint (\cos\left[\frac{\bar{k}}{\Theta} \cdot \left(\frac{\bar{X}_1}{|\bar{X}_1|^3} + \frac{\bar{X}_2}{|\bar{X}_2|^3}\right)\right] - 1\right) G_A d\bar{X}_1 d\bar{X}_2 \right. \right. \\
&\quad \left. \left. + \iint (\cos\left[\frac{\bar{k}}{\Theta} \cdot \left(\frac{\bar{X}_1}{|\bar{X}_1|^3} - \frac{\bar{X}_2}{|\bar{X}_2|^3}\right)\right] - 1\right) G_B d\bar{X}_1 d\bar{X}_2 \right\} \right]. \tag{6.6}
\end{aligned}$$

Since the term \bar{k}/Θ keeps occurring in Eq.(6.5) and Eq.(6.6), we make one final change, writing

$$\bar{l} \equiv \frac{\bar{k}}{\Theta},$$

thereby giving us the final result

$$\begin{aligned}
F(\bar{l}) &= F_0(\bar{l}) F_1(\bar{l}) \\
&= \exp\left[-\frac{4}{5} \bar{l}^{3/2} (2\pi)^{1/2}\right] \\
&\quad \times \exp\left[\left(\frac{3}{4\pi}\right)^2 \left\{ \iint (\cos\left[\bar{l} \cdot \left(\frac{\bar{X}_1}{|\bar{X}_1|^3} + \frac{\bar{X}_2}{|\bar{X}_2|^3}\right)\right] - 1\right) \right. \right. \\
&\quad \left. \left. \times G_A d\bar{X}_1 d\bar{X}_2 + \iint (\cos\left[\bar{l} \cdot \left(\frac{\bar{X}_1}{|\bar{X}_1|^3} - \frac{\bar{X}_2}{|\bar{X}_2|^3}\right)\right] - 1\right) G_B d\bar{X}_1 d\bar{X}_2 \right\} \right]. \tag{6.7}
\end{aligned}$$

Note that Eq.(6.7) is just the same as Eq.(4.5), except for the fact that we will now calculate $P(\bar{\mathbf{E}})$ instead of $P(\bar{E})$. This merely amounts to multiplying \bar{E} by the constant $\frac{ea}{k_0 T}$, so there is no fundamental difference between Eq.(4.5) and Eq.(6.7).

CHAPTER III

EVALUATION OF THE KELBG INTEGRALS

7 The Monte Carlo Method

We have now progressed to the point where the evaluation of $P(\bar{\epsilon})$ depends on our ability to solve integrals of the form

$$I_A(\bar{\epsilon}) \equiv \int \cdots \int (\cos(B) - 1) G_A(\bar{x}_1, \bar{x}_2) d\bar{x}_1 d\bar{x}_2 \quad (7.1)$$

which occur in

$$F(\bar{\epsilon}) = \exp\left[-\frac{4\bar{\epsilon}^{3/2}}{5} (2\pi)^{1/2}\right] \exp\left[\frac{9}{16\pi}(I_A + I_B)\right], \quad (7.2)$$

where

$$B \equiv \bar{\epsilon} \cdot \left(\frac{\bar{x}_1}{|\bar{x}_1|^3} + \frac{\bar{x}_2}{|\bar{x}_2|^3} \right) \cdot$$

Since $G(\bar{x}_1, \bar{x}_2)$ is a tabulated function, the analytical form of which we do not know,¹⁷ it would be very difficult for us to evaluate Eq.(7.1) analytically. We therefore turn to the numerical method outlined in Appendix C. This technique, called the "Monte Carlo Method," has been explored by several authors,¹⁸⁻²¹ so, as in Appendix C, we shall discuss it here only in operational terms as it affects the evaluation of Eq.(7.1).

To apply this method to the six dimensional integrals at hand we simply note that Eq.(7.1) is in the form

$$I = \int \cdots \int F(\bar{x}_1, \bar{x}_2) G(\bar{x}_1, \bar{x}_2) d\bar{x}_1 d\bar{x}_2$$

which is a six dimensional analogue of Eq.(C.1). Thus, following the procedure outlined in Appendix C, we define a probability

distribution $P(\bar{X}_1, \bar{X}_2)$ as

$$P(\bar{X}_1, \bar{X}_2) = \frac{F(\bar{X}_1, \bar{X}_2)}{\int \dots \int F(\bar{X}_1, \bar{X}_2) d\bar{X}_1 d\bar{X}_2}, \quad (7.3)$$

and write

$$\begin{aligned} I(\bar{e}) &= \left\{ \int \dots \int F(\bar{X}_1, \bar{X}_2) d\bar{X}_1 d\bar{X}_2 \right\} \int \dots \int P(\bar{X}_1, \bar{X}_2) G(\bar{X}_1, \bar{X}_2) d\bar{X}_1 d\bar{X}_2 \\ &= \left\{ \int \dots \int F(\bar{X}_1, \bar{X}_2) d\bar{X}_1 d\bar{X}_2 \right\} \langle G(\bar{X}_1, \bar{X}_2) \rangle \end{aligned}$$

Now if $P(\bar{X}_1, \bar{X}_2)$ is a properly normalized probability function, it is required that²²

$$0 \leq P(\bar{X}_1, \bar{X}_2),$$

and

$$\int \dots \int P(\bar{X}_1, \bar{X}_2) d\bar{X}_1 d\bar{X}_2 = 1.$$

Thus $F(\bar{X}_1, \bar{X}_2)$ must always be greater than zero. Also $\int \dots \int F d\bar{X}_1 d\bar{X}_2$ must be a real, finite, positive number, and naturally this integral must be "solvable". To meet these conditions we note that $F(\bar{X}_1, \bar{X}_2)$ cannot be written as $\cos(B) - 1$ (see Eq.(7.1)), since this can be negative. We therefore rewrite Eq.(7.1) in the form

$$I_A(\bar{e}) = - \int \dots \int (1 - \cos(B)) G_A d\bar{X}_1 d\bar{X}_2, \quad (7.4)$$

resulting in

$$F(\bar{X}_1, \bar{X}_2) = 1 - \cos(B). \quad (7.5)$$

If we attempt to normalize Eq.(7.5), as in Eq.(7.3), the normalizing constant,

$$\int \dots \int F(\bar{X}_1, \bar{X}_2) d\bar{X}_1 d\bar{X}_2,$$

is not finite, since the integral diverges. Thus if we want

to put our equations in a form for a Monte Carlo calculation, $F(\bar{X}_1, \bar{X}_2)$ must be modified. It may be, for example, that we could find a function, $H(\bar{X}_1, \bar{X}_2)$, such that $H(\bar{X}_1, \bar{X}_2) F(\bar{X}_1, \bar{X}_2)$ would go to zero rapidly, if $|\bar{X}_1|$ or $|\bar{X}_2|$ got large. This not only would give us the convergence we require, but it might also effectively reduce the space over which we must integrate, thereby allowing us to evaluate the integrals with fewer points. Our problem in this regard is compounded by the fact that if we modify $F(\bar{X}_1, \bar{X}_2)$ we will also have to modify $G(\bar{X}_1, \bar{X}_2)$, as shown in Appendix C. And, as was also indicated there, the modified term, $H^{-1}(\bar{X}_1, \bar{X}_2) G(\bar{X}_1, \bar{X}_2)$, should be as slowly varying as possible, so that we need use as few points as possible in the evaluation of the integral. Thus any function $H(\bar{X}_1, \bar{X}_2)$ that we use to modify Eq.(7.5) must be carefully chosen if all of the above conditions are to be met.

8 The Function $\exp(-|\bar{X}_1|^2 - |\bar{X}_2|^2)$

The choice of an H is a difficult one since we do not know the functional form of G. However, one obvious way to make P, Eq.(7.3), go to zero if either $|\bar{X}_1|$ or $|\bar{X}_2|$ gets large is to write

$$F'(\bar{X}_1, \bar{X}_2) = \exp[-|\bar{X}_1|^2 - |\bar{X}_2|^2] [1 - \cos(\theta)] \cdot \quad (8.1)$$

Thus

$$P(\bar{X}_1, \bar{X}_2) = \frac{e^{-|\bar{X}_1|^2 - |\bar{X}_2|^2} [1 - \cos(\theta)]}{\int \dots \int e^{-|\bar{X}_1|^2 - |\bar{X}_2|^2} [1 - \cos(\theta)] d\bar{X}_1 d\bar{X}_2}$$

and

$$G'(\bar{x}_1, \bar{x}_2) = \exp[|\bar{x}_1|^2 + |\bar{x}_2|^2] G_A(\bar{x}_1, \bar{x}_2),$$

giving

$$I_A = \left\{ \dots \int F'(\bar{x}_1, \bar{x}_2) d\bar{x}_1 d\bar{x}_2 \right\} \langle G'(\bar{x}_1, \bar{x}_2) \rangle. \quad (8.2)$$

Now the integral

$$\int \dots \int F'(\bar{x}_1, \bar{x}_2) d\bar{x}_1 d\bar{x}_2$$

can be evaluated as

$$\pi^3 - \left(\frac{4\pi}{\ell}\right)^2 Q(\ell), \quad (8.3)$$

where

$$Q(\ell) \equiv \int_0^{\infty} r^4 e^{-r^2} \sin\left[\frac{\ell}{r^2}\right] dr. \quad (8.4)$$

Eq.(8.4) is solved via a Simpson's rule calculation²³ on the IBM 1620 computer, the details of which are given in Appendix D. Clearly, then, P, as defined in this section, satisfies all of the requirements of a probability distribution. Therefore we can use it to calculate $\langle G'_A \rangle$ for a particular value of the parameter ℓ . (See Appendix E for an explanation of the computer program used here.)

Tables I-III list the results of these calculations for the two step lengths and starting points used as indicated (see Appendix C). Also given are the numbers of times the particles failed to move, as explained in Appendix C, and this shows clearly the effect of changing the step length.

This data is presented graphically in Figure 1, in which curve I corresponds to Table I, etc. Note that curves I and II

Table I. Monte Carlo calculation of $\langle G'(\bar{X}_1, \bar{X}_2) \rangle$, where

$$G'(\bar{X}_1, \bar{X}_2) = \exp[-|\bar{X}_1|^2 - |\bar{X}_2|^2] G_A(\bar{X}_1, \bar{X}_2).$$

Step Length: 0.3a. Starting Point: $x_1 = .730260$, $x_2 = .453186$,
 $y_1 = .445617$, $y_2 = -.080333$, $z_1 = .423193$, $z_2 = .251065$.

Number of Points in Units of 100	Number of Times Particles Failed to Move	$G'(\bar{X}_1, \bar{X}_2)$
1	54	-.856069
2	101	-.718523
3	137	-1.027242
4	194	-.908586
5	240	-1.341609
6	298	-1.161375
7	358	-1.049808
8	418	-.971139
9	477	-.902549
10	523	-.843671
11	579	-.808534
12	634	-.801743
13	695	-.764932
14	751	-.753454
15	800	-.756087
16	854	-.747455
17	915	-.721369
18	967	-.711488
19	1013	-.693245
20	1062	-.678147
21	1121	-.660293
22	1168	-.648782
23	1213	-.644537
24	1264	-.639816
25	1316	-.629133

Table II. Monte Carlo calculation of $\langle G'(\bar{X}_1, \bar{X}_2) \rangle$, where

$$G'(\bar{X}_1, \bar{X}_2) = \exp[+|\bar{X}_1|^2 + |\bar{X}_2|^2] G_A(\bar{X}_1, \bar{X}_2).$$

Step Length: 0.3a. Starting Point: $x_1 = .233324$, $x_2 = .283296$,
 $y_1 = .063209$, $y_2 = -.089085$, $z_1 = .452913$, $z_2 = .446226$.

Number of Points In Units of 100	Number of Times Particles Failed to Move	$G'(\bar{X}_1, \bar{X}_2)$
1	63	-.460805
2	113	-.378514
3	171	-.354120
4	230	-.336638
5	279	-.364649
6	342	-.350849
7	405	-.339125
8	466	-.336208
9	525	-.345720
10	570	-.378879
11	633	-.381811
12	680	-.395412
13	722	-.390185
14	783	-.391491

Table III. Monte Carlo calculation of $\langle G'(\bar{x}_1, \bar{x}_2) \rangle$, where

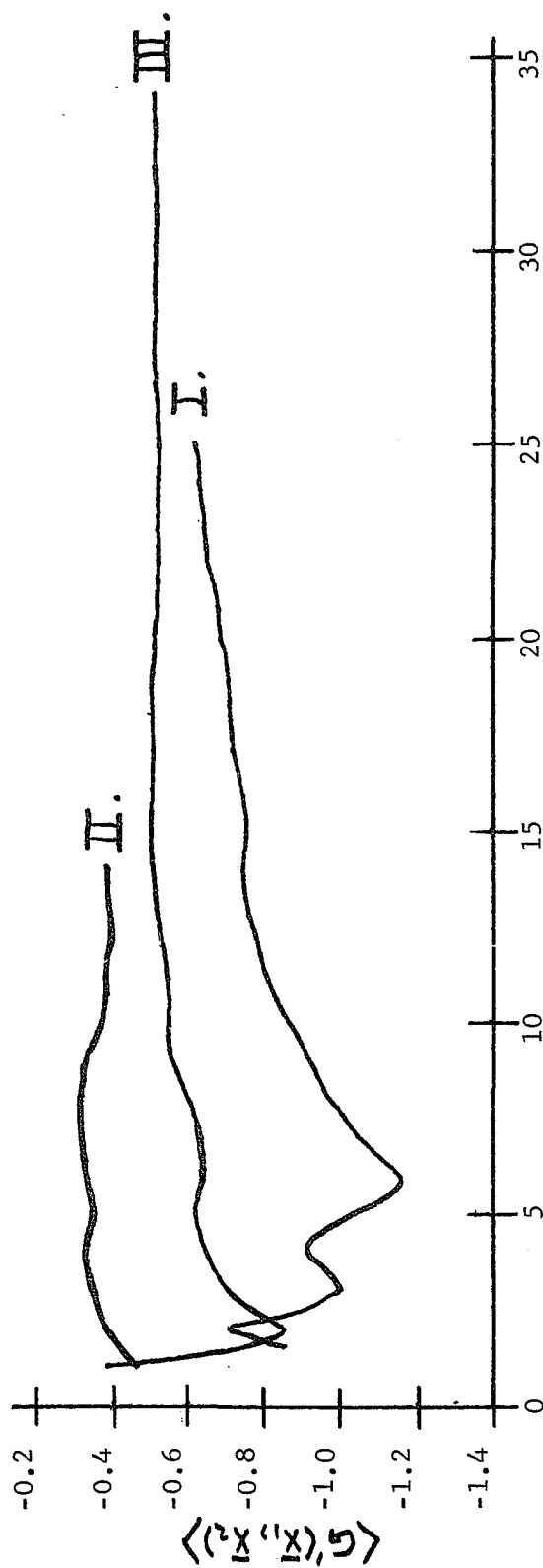
$$G'(\bar{x}_1, \bar{x}_2) = \exp[-(|\bar{x}_1|^2 + |\bar{x}_2|^2)] G_A(\bar{x}_1, \bar{x}_2).$$

Step Length: 0.5a. Starting Point: $x_1 = .233324$, $x_2 = .283296$,
 $y_1 = .063209$, $y_2 = -.089085$, $z_1 = .452913$, $z_2 = .446226$.

Number of Points in Units of 100	Number of Times Particles Failed to Move	$G'(\bar{x}_1, \bar{x}_2)$
1	69	-.398466
2	144	-.837358
3	217	-.710722
4	294	-.632067
5	362	-.617953
6	433	-.643368
7	517	-.636353
8	588	-.603364
9	674	-.567420
10	746	-.557411
11	816	-.544317
12	901	-.524384
13	976	-.510393
14	1047	-.508626
15	1121	-.505374
16	1195	-.513994
17	1274	-.501182
18	1344	-.497116
19	1414	-.509803
20	1488	-.514241
21	1560	-.514550
22	1626	-.525519
23	1694	-.519875
24	1767	-.523368
25	1829	-.526026
26	1911	-.519455
27	1985	-.514515
28	2055	-.515968
29	2126	-.521450
30	2198	-.528565
31	2279	-.520496
32	2345	-.517648
33	2413	-.520625
34	2473	-.529732

Monte Carlo calculation of $\langle G(\bar{x}_1, \bar{x}_2) \rangle$, where

$$G(\bar{x}_1, \bar{x}_2) = \exp [|\bar{x}_1|^2 + |\bar{x}_2|^2] G_A(\bar{x}_1, \bar{x}_2).$$



Steps in Units of 100

Figure 1

have the same step length, but the starting point for curve II is the finishing point of curve I. Thus curve II is really just an extension of curve I, and if we had allowed curve I to simply continue, instead of stopping and starting over with its terminal point as the new starting point, it would have approached curve III. It seems, then, that there are at least two regions in the space which give quite different values for G' . One of these seems to be at $G' \approx 0.39$, with another at G' larger than 0.8. The evaluation points jump back and forth between these regions, and $\langle G' \rangle$ would eventually approach the proper value.

Now in curve III we see a rather consistent behavior, compared with curve I. Note also that the Monte Carlo evaluation which led to curve III had the same starting point as that which led to curve II, although the step length was lengthened for curve III. Thus it is not surprising that curves II and III start, after one hundred points, with similar values for $\langle G' \rangle$. The important thing, however, is the fact that curve III is, after some initial fluctuation, quite constant. This may be the result of taking a longer step length, thereby allowing the various regions in space to be sampled more consistently. With the longer step length, however, the evaluation points move only about 25% of the time, while they move 48% of the time with the shorter step length. This may or may not be important, but we are inclined to think that it is not, since the first two curves approach the third anyway.

In this section we have shown one solution for Eq.(7.1). The value of the parameters used here are those that shall be used throughout the remainder of this work. They are

$$\begin{aligned} \ell &= \frac{\pi}{10} , \\ \theta &= 4.0 \end{aligned} \quad (8.5)$$

and

$$\sigma = 0.5 .$$

Note that we would have to make similar runs for every value of ℓ , and we would also have to evaluate $I_B(\bar{\ell})$, as indicated in Eq.(7.1), for all points in ℓ -space, before $P(\bar{\epsilon})$ could finally be calculated for the θ , and σ given above. Note also that our Monte Carlo evaluation has only given us $\langle G' \rangle$, and that we must also evaluate Eq.(8.3) before we know $I_A(\bar{\ell})$. This has been done for $\ell = \pi/10$, and thus, if we choose $\langle G' \rangle = -.52$ as the best choice from the Monte Carlo evaluation, we may write

$$\begin{aligned} I_A\left(\frac{\pi}{10}\right) &= \left\{ \pi^3 - \left(\frac{4\pi}{\pi/10}\right)^2 (0.1283)^2 \right\} (-0.52) \\ &= -2.44 , \end{aligned} \quad (8.6)$$

where $d(\pi/10) = .1283$ from Appendix D.

9 The Function $\cos(\varphi_1 - \varphi_2)$

If one could eliminate all of the "oscillations" that $\langle G \rangle$ goes through in Figure 1, the amount of computer time needed to evaluate $I_A(\bar{\ell})$, and thereby $F(\bar{\ell})$, would be reduced. For

example we can see that in curve III, of Figure 1, fully 1300 points had to be taken before the function "settled down," and even after that one might argue that the rather stable behavior of the curve could break down at any time, thereby eroding confidence in the final value, of $\langle G' \rangle = -.52$, taken from Figure 1.

To attack this problem we first note that the fluctuations are probably caused by the nature of the function $G_A = g_A - 1$. A graph of G_A is given in Figure 2, as a function of the particle separation, in units of our length parameter a , and we see that at a particle separation of $0.4a$ there is a sharp discontinuity in G_A , caused by the hard sphere assumption.¹⁷ This discontinuity probably contributes greatly to the form of Figure 1, and we shall try then to eliminate its effect as much as possible.

In order to accomplish this we shall look for functions which will be a minimum when the particle separation becomes small, and the first ones we shall try involve the term $\cos(\varphi_1 - \varphi_2)$. When the particle separation, $|\bar{X}_1 - \bar{X}_2|$, is small the chances are good that $\varphi_1 \sim \varphi_2$, and $\cos(\varphi_1 - \varphi_2) \sim 1$. When $|\bar{X}_1 - \bar{X}_2|$ is large, however, φ_1 may or may not be close to φ_2 , but this is not so important since the problem is only at small particle separations. Thus if we write

$$G'(\bar{X}_1, \bar{X}_2) \equiv \frac{G_A(\bar{X}_1, \bar{X}_2) \exp[|\bar{X}_1|^2 + |\bar{X}_2|^2]}{[N - \frac{D}{N}]},$$

where

$$D \equiv |\bar{X}_1|^2 + |\bar{X}_2|^2 - 2|\bar{X}_1||\bar{X}_2|\cos(\varphi_1 - \varphi_2),$$

The Function $G_A = \xi_A - 1$, for $\phi = 4.0$, and $\sigma = 0.4$.

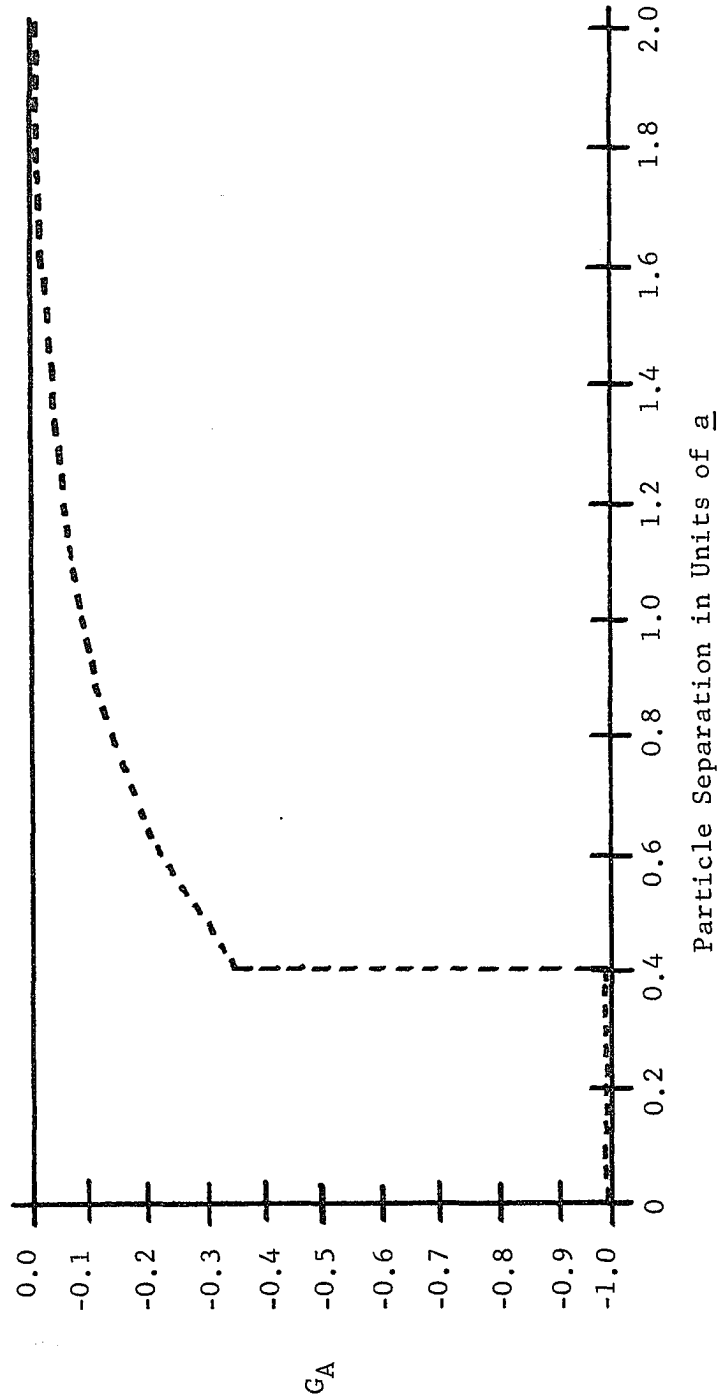


Figure 2

and if we choose $N = 10$ to keep $(N - \frac{D}{N})$ positive, then G' will be reduced when $\cos(\varphi_1 - \varphi_2)$ approaches its maximum value, i.e. when $\varphi_1 \rightarrow \varphi_2$, thereby smoothing out the step at 0.4a.

Using this function we have

$$F'(\bar{x}_1, \bar{x}_2) = [N - \frac{D}{N}] \exp[-|\bar{x}_1|^2 - |\bar{x}_2|^2] [1 - \cos(B)],$$

where again we define

$$B \equiv \ell \cdot \left[\frac{\bar{x}_1}{|\bar{x}_1|^3} + \frac{\bar{x}_2}{|\bar{x}_2|^3} \right].$$

Thus

$$\begin{aligned} & \int \dots \int F'(\bar{x}_1, \bar{x}_2) d\bar{x}_1 d\bar{x}_2 \\ &= 10 \left[\pi^3 - \left(\frac{4\pi}{\ell} \right)^2 d(\ell) \right] - 0.1 \left[3\pi^3 - \frac{32\pi^2}{\ell^2} d(\ell) d'(\ell) \right], \end{aligned}$$

with

$$d'(\ell) = \left\{ \int_0^\infty r^6 e^{-r^2} \sin\left[\frac{\ell}{r^2}\right] dr \right\}^2. \quad (9.1)$$

Now Eq.(9.1) is solved by a Simpson's rule calculation just as Eq.(8.4) was, and for $\ell = \pi/10$ we have $Q'(\pi/10) = .2058$. With this we can write down the equation

$$I_A\left(\frac{\pi}{10}\right) = 45.9786 \langle G'(\bar{x}_1, \bar{x}_2) \rangle, \quad (9.2)$$

and turn to the solution of $\langle G'(\bar{x}_1, \bar{x}_2) \rangle$.

This solution is accomplished in the same manner as before, and the results are given in Table IV, and are plotted in Figure 3. We see that the curve is slowly varying in comparison with those of Figure 1. Thus we might hope that our objective in this regard has been accomplished. However we have only made a Monte Carlo

Table IV. Monte Carlo calculation of $\langle G'(\bar{X}_1, \bar{X}_2) \rangle$, where

$$G'(\bar{x}_1, \bar{x}_2) = \exp[-(\bar{x}_1^2 + \bar{x}_2^2)] G_A(\bar{x}_1, \bar{x}_2) / [N - \frac{D}{N}].$$

Step Length: 0.3a. Starting Point: $x_1 = .233324$, $x_2 = .283296$,
 $y_1 = .063209$, $y_2 = -.089085$, $z_1 = .452913$, $z_2 = .446226$.

Number of Points in Units of 100	Number of Times Particles Failed to Move	$G'(\bar{X}_1, \bar{X}_2)$
1	63	-.046525
2	113	-.038213
3	158	-.037083
4	213	-.035733
5	277	-.038213
6	344	-.038495
7	400	-.038761
8	461	-.039484

Monte Carlo calculation of $\langle G'(\bar{x}_1, \bar{x}_2) \rangle$, where

$$G'(\bar{x}_1, \bar{x}_2) = \exp[-\lambda(\bar{x}_1^2 + \bar{x}_2^2)] G_A(\bar{x}_1, \bar{x}_2) / [N - \frac{D}{N}] .$$

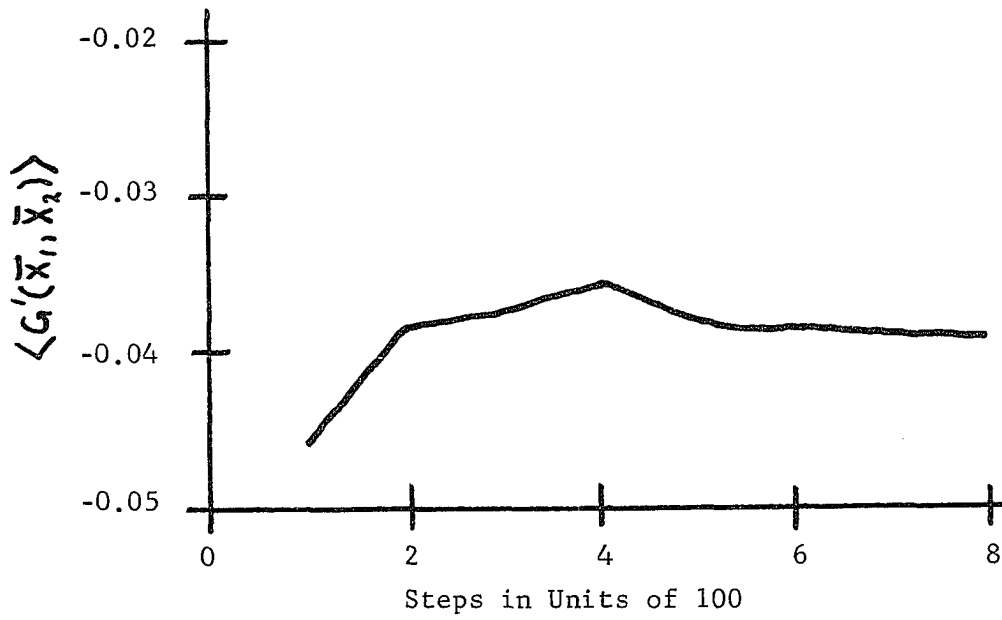


Figure 3

run of 800 points because this new function takes three times as much computer time to evaluate as does the function in section 8. It could be, then, that if we had run for a longer while some oscillation would have occurred. Hence this new function does not leave us feeling too confident, since we have not really explored it as thoroughly as we have the others. However we can compare this result with that of Eq.(8.6) by completing Eq.(9.2), giving

$$I_A\left(\frac{\pi}{10}\right) = -1.82, \quad (9.3)$$

where we have chosen as the value for $\langle G'(\bar{X}_1, \bar{X}_2) \rangle$, $-.039$.

This value of $I_A(\pi/10)$ is 25% higher than that obtained in section 8, so we see that these two methods are close to agreement, and presumably if we could have run a little longer with both of them the agreement could have gotten even better. Thus our confidence, at least in the consistency of our methods, is strengthened, and we are encouraged to try yet another modification of Eq.(8.1).

This time we shall also use a function involving $\cos(\varphi_1 - \varphi_2)$, but in a simpler expression which, hopefully, will not take up so much computer time. Our new function is simply $1 + \cos(\varphi_1 - \varphi_2)$, giving

$$F(\bar{X}_1, \bar{X}_2) = [1 + \cos(\varphi_1 - \varphi_2)] \exp[-|\bar{X}_1|^2 - |\bar{X}_2|^2] [1 - \cos(B)].$$

Hence

$$\int \cdots \int F(\bar{X}_1, \bar{X}_2) d\bar{X}_1 d\bar{X}_2 = \pi^3 - \left(\frac{4\pi}{e}\right)^2 \mathcal{L}^2(e)$$

just as in Eq.(8.3), and

$$G'(\bar{X}_1, \bar{X}_2) = \frac{\exp[|\bar{X}_1|^2 + |\bar{X}_2|^2] G_A(\bar{X}_1, \bar{X}_2)}{[1 + \cos(\varphi_1 - \varphi_2)]} . \quad (9.4)$$

Thus we have

$$I_A\left(\frac{\pi}{10}\right) = 4.6833 \langle G'(\bar{X}_1, \bar{X}_2) \rangle , \quad (9.5)$$

where G' is now defined by Eq.(9.4), and $P(\bar{X}_1, \bar{X}_2)$ in the integral, Eq.(7.3), involves the functions defined above.

The results of the Monte Carlo evaluation of $\langle G'(\bar{X}_1, \bar{X}_2) \rangle$ are given in Tables V-VII, and in Figure 4, for the various step lengths and starting points indicated in the Tables. We see that the oscillations in $\langle G'(\bar{X}_1, \bar{X}_2) \rangle$ are still with us, and it is almost impossible from Figure 4 to tell what the average value of the function really is, since we did not take enough points. If we select $\langle G'(\bar{X}_1, \bar{X}_2) \rangle = -0.69$, from curve V, then Eq.(9.5) gives us

$$I_A\left(\frac{\pi}{10}\right) = -3.23 , \quad (9.6)$$

which is about 25% and 44% lower than the other two values for $I_A(\pi/10)$ respectively.

For the first and third evaluations of $I_A(\pi/10)$, the Monte Carlo runs took about eight minutes for every hundred points taken. The second evaluation, using the function $\left[N - \frac{D}{N} \right]$, required about twenty-two minutes per hundred points. Thus this third function has improved the time factor, over the second, but it has failed to improve upon the consistency of the first function, and in fact may be even more wildly varying. The reason may be because the denominator of G' can go to zero, thereby causing G' to

Table V. Monte Carlo calculation of $\langle G'(\bar{X}_1, \bar{X}_2) \rangle$, where

$$G'(\bar{X}_1, \bar{X}_2) = \exp[|\bar{X}_1|^2 + |\bar{X}_2|^2] G_A(\bar{X}_1, \bar{X}_2) / [1 + \cos(\varphi_1 - \varphi_2)].$$

Step Length: 0.3a. Starting Point: $x_1 = .2333324$, $x_2 = .283296$,
 $y_1 = .063209$, $y_2 = -.089085$, $z_1 = .452913$, $z_2 = .446226$.

Number of Points in Units of 100	Number of Times Particles Failed to Move	$G'(\bar{X}_1, \bar{X}_2)$
1	63	-.391364
2	120	-.441954
3	182	-.434767
4	249	-.420812
5	290	-.495487
6	345	-.500780
7	395	-.587413
8	438	-.632507
9	485	-.611214
10	549	-.604278
11	601	-.648120
12	653	-1.073069
13	709	-1.073620
14	775	-1.026503
15	837	-.983108
16	894	-.954056
17	963	-.926716
18	1038	-.884736
19	1093	-.864095
20	1158	-.840733
21	1223	-.815911
22	1278	-.799742
23	1339	-.787946
24	1393	-.773363
25	1447	-.772515
26	1500	-.760686
27	1556	-.751144
28	1608	-.763789
29	1669	-.762782
30	1725	-.753234
31	1768	-.749218
32	1833	-.735783
33	1906	-.724123
34	1960	-.712428
35	2009	-.708915
36	2066	-.717261
37	2132	-.710341
38	2194	-.701924

Table V. Continued

39	2267	-.690333
40	2320	-.697482
41	2380	-.688840
42	2433	-.681820

Table VI. Monte Carlo calculation of $\langle G'(\bar{X}_1, \bar{X}_2) \rangle$, where

$$G'(\bar{X}_1, \bar{X}_2) = \exp[|\bar{X}_1|^2 + |\bar{X}_2|^2] G_A(\bar{X}_1, \bar{X}_2) / [1 + \cos(\varphi_1 - \varphi_2)] \cdot$$

Step Length: 0.3a. Starting Point: $x_1 = .533946$, $x_2 = -.009074$,
 $y_1 = -.042777$, $y_2 = -.358963$, $z_1 = .546538$, $z_2 = .406052$.

Number of Points in Units of 100	Number of Times Particles Failed to Move	$G'(\bar{X}_1, \bar{X}_2)$
1	61	-.351537
2	137	-.378586
3	209	-.766463
4	282	-1.002559
5	338	-.864042
6	393	-.805570
7	444	-.787359
8	492	-.767933
9	555	-.719984
10	622	-.682169
11	670	-.687069
12	727	-.729262
13	802	-.701553
14	862	-.681224
15	906	-.763590

Table VII. Monte Carlo calculations of $\langle G'(\bar{x}_1, \bar{x}_2) \rangle$, where

$$G'(\bar{x}_1, \bar{x}_2) = \exp[|\bar{x}_1|^2 + |\bar{x}_2|^2] G_A(\bar{x}_1, \bar{x}_2) / [1 + \cos(\varphi_1 - \varphi_2)].$$

Step Length: 0.4a. Starting Point: $x_1 = .533946$, $x_2 = -.009074$,
 $y_1 = -.042777$, $y_2 = -.358963$, $z_1 = .546538$, $z_2 = .406052$.

Number of Points in Units of 100	Number of Times Particles Failed to Move	$G'(\bar{x}_1, \bar{x}_2)$
1	79	-.585734
2	148	-.416910
3	194	-1.205509
4	264	-1.025993
5	334	-.889085
6	416	-.812842
7	484	-.747090
8	544	-.724571
9	607	-.821318
10	669	-.790463
11	734	-.760627
12	802	-.741753
13	862	-.736566
14	920	-.899169
15	980	-1.037172

Monte Carlo calculation of $\langle G(\bar{x}_1, \bar{x}_2) \rangle$, where

$$G(\bar{x}_1, \bar{x}_2) = \frac{\exp[-\bar{x}_1^2 - |\bar{x}_2|^2] G_A(\bar{x}_1, \bar{x}_2)}{[1 + \cos(\varphi_1 - \varphi_2)]}$$

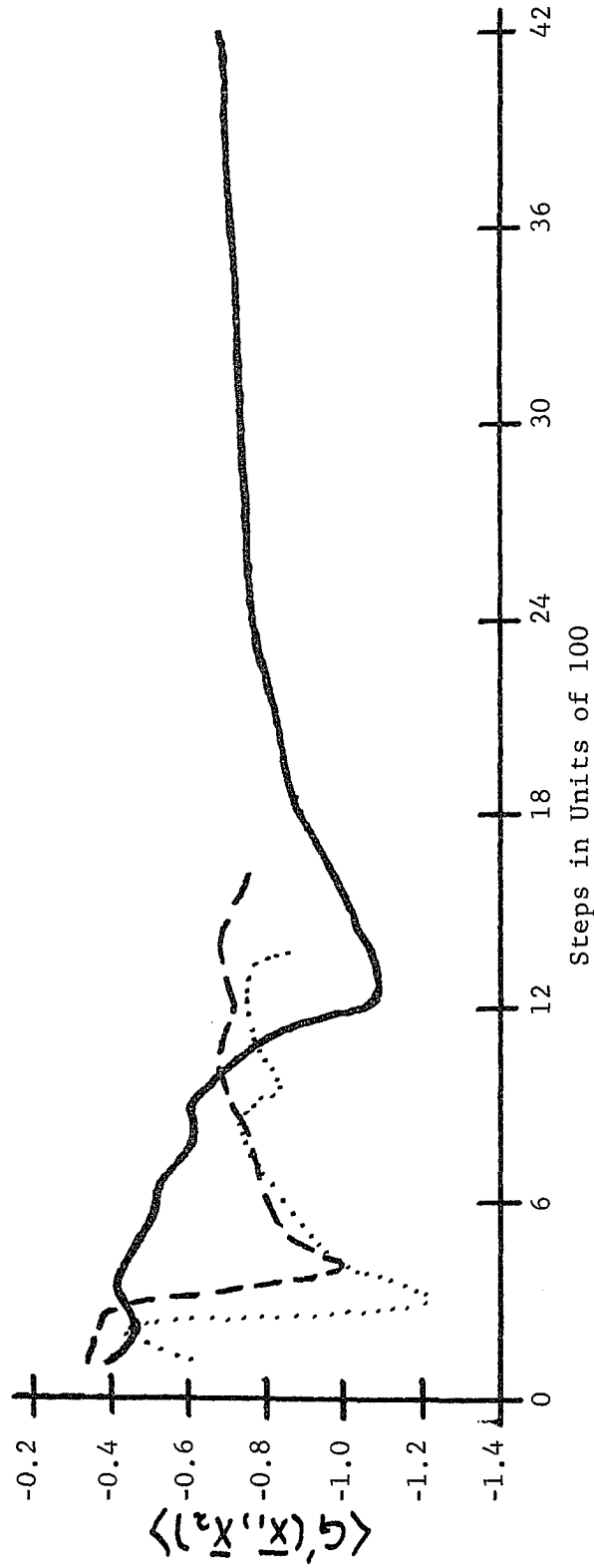


Figure 4

become extremely large. This introduces the very kind of large fluctuation we had hoped to eliminate.

10 The Function $\exp[-|\bar{x}_1 - \bar{x}_2|^2]$

The reason for using the function $\cos(\varphi_1 - \varphi_2)$ in the last section was so that the effect of the discontinuity in G_A on $\langle G' \rangle$ could be minimized. But the results were poor, so in this section we turn to another function, that being

$$H(\bar{x}_1, \bar{x}_2) = \exp[-|\bar{x}_1|^2 - |\bar{x}_2|^2] \exp[-|\bar{x}_1 - \bar{x}_2|^2].$$

This function will give

$$G'(\bar{x}_1, \bar{x}_2) = \exp[|\bar{x}_1|^2 + |\bar{x}_2|^2 + |\bar{x}_1 - \bar{x}_2|^2] G_A(\bar{x}_1, \bar{x}_2),$$

which should not be nearly so wildly varying as before, since for small particle separations, where G_A jumps to -1, $\exp[|\bar{x}_1 - \bar{x}_2|^2]$ will get very small. This is because $|\bar{x}_1 - \bar{x}_2|^2$ is the square of the particle separation itself. Thus instead of involving only two coordinates in the separation correlation of G' , we have included the entire particle separation function.

Now we first write

$$F'(\bar{x}_1, \bar{x}_2) = \exp[-|\bar{x}_1|^2 - |\bar{x}_2|^2 - |\bar{x}_1 - \bar{x}_2|^2] [1 - \cos(B)],$$

where B is as defined earlier. But the integral

$$\int \dots \int F'(\bar{x}_1, \bar{x}_2) d\bar{x}_1 d\bar{x}_2$$

is very difficult to solve analytically, so we are led to make a change. Let us write, then,

and

$$G'(\bar{x}_1, \bar{x}_2) = [1 - \cos(\theta)] G_A(\bar{x}_1, \bar{x}_2) \exp[|\bar{x}_1|^2 + |\bar{x}_2|^2 + |\bar{x}_1 - \bar{x}_2|^2],$$

$$F'(\bar{x}_1, \bar{x}_2) = \exp[-|\bar{x}_1|^2 - |\bar{x}_2|^2 - |\bar{x}_1 - \bar{x}_2|^2].$$

Note that this immediately gives us an unexpected bonus, because

$$\int \dots \int F'(\bar{x}_1, \bar{x}_2) d\bar{x}_1 d\bar{x}_2 \quad (10.1)$$

and, therefore $P(\bar{x}_1, \bar{x}_2)$, is independent of the parameter ℓ .

That means we need only make one Monte Carlo run for all of the integrals $I_A(\bar{\ell})$, which in itself is a great savings. Thus we note that Eq.(10.1) is equal to

$$\int \dots \int e^{-|\bar{x}_1|^2 - |\bar{x}_2|^2 - |\bar{x}_1 - \bar{x}_2|^2} d\bar{x}_1 d\bar{x}_2 = 5.94.$$

Now we have

$$I_A(\bar{\ell}) = 5.94 \langle G'(\bar{x}_1, \bar{x}_2, \ell) \rangle, \quad (10.2)$$

and the results of the Monte Carlo calculation, for $\ell = (\pi/10)$, are given in Table VIII and Figure 5.

The oscillations are still very much with us, although a longer step length in the Monte Carlo calculation might be cut down on them just as it did in curve III of Figure 1. Note that for $\ell = (\pi/10)$, if we assume $\langle G'(\bar{x}_1, \bar{x}_2, (\pi/10)) \rangle = -0.655$, we have

$$I_A\left(\frac{\pi}{10}\right) = -3.89 \quad (10.3)$$

which is about 37%, 53%, and 17% lower than the other calculated values respectively. Note also that with a longer run, $\langle G'(\bar{x}_1, \bar{x}_2, (\pi/10)) \rangle$ might have gotten smaller, (see Figure 5), although this is not certain. But if it had, the agreement with the other values would have been improved.

Table VIII. Monte Carlo calculation of $\langle G'(\bar{X}_1, \bar{X}_2) \rangle$, where

$$G'(\bar{X}_1, \bar{X}_2) = \exp[-(|\bar{X}_1|^2 + |\bar{X}_2|^2 + |\bar{X}_1 - \bar{X}_2|^2)] G_A(\bar{X}_1, \bar{X}_2).$$

Step Length: 0.4a. Starting Point: $x_1 = .111090$, $x_2 = .623079$,
 $y_1 = -.654167$, $y_2 = -.985409$, $z_1 = -.024385$, $z_2 = .290268$.

Number of Points in Units of 100	Number of Times Particles Failed to Move	$G'(\bar{X}_1, \bar{X}_2)$
1	37	-.220369
2	68	-.325184
3	114	-.359629
4	160	-.351531
5	198	-.406762
6	240	-.422512
7	286	-.423250
8	333	-.415047
9	367	-.401537
10	411	-.448449
11	452	-.433320
12	497	-.412912
13	545	-.427313
14	589	-.418461
15	635	-.409141
16	684	-.400359
17	720	-.396663
18	770	-.398270
19	806	-.405884
20	854	-.395462
21	897	-.449646
22	939	-.471606
23	982	-.505290
24	1018	-.505532
25	1065	-.499064
26	1112	-.493518
27	1143	-.525553
28	1180	-.517703
29	1217	-.513867
30	1264	-.501939
31	1308	-.494651
32	1363	-.499761
33	1415	-.491778
34	1456	-.522101
35	1500	-.516013
36	1544	-.509852
37	1595	-.502810
38	1641	-.501308

Table VIII. Continued

39	1681	-.500700
40	1718	-.495702
41	1759	-.487612
42	1803	-.493437
43	1842	-.486631
44	1885	-.479031
45	1927	-.484796
46	1969	-.483723
47	2014	-.479333
48	2047	-.887118
49	2088	-.878817
50	2132	-.868986
51	2182	-.867699
52	2215	-.858678
53	2249	-.856530
54	2295	-.845410
55	2337	-.835691
56	2383	-.828540
57	2428	-.820339
58	2471	-.814228
59	2511	-.812996
60	2555	-.805277
61	2591	-.798579
62	2624	-.794273
63	2669	-.804382
64	2706	-.799270
65	2746	-.788698
66	2786	-.780665
67	2833	-.775085
68	2871	-.766132
69	2907	-.761239
70	2943	-.754477
71	2992	-.750423
72	3031	-.742587
73	3071	-.738536
74	3112	-.734218
75	3155	-.732669
76	3191	-.725700
77	3237	-.728508
78	3285	-.726858
79	3325	-.724920
80	3356	-.720863
81	3396	-.717177
82	3437	-.715735
83	3473	-.710011
84	3510	-.704815
85	3559	-.699279
86	3602	-.696741

Table VIII. Continued

87	3642	-.695052
88	3683	-.691570
89	3707	-.689239
90	3747	-.684957
91	3788	-.682203
92	3837	-.677702
93	3883	-.676104
94	3926	-.674071
95	3967	-.669914
96	4018	-.666881
97	4054	-.662676
98	4083	-.657629
99	4234	-.656284
100	4173	-.652223
101	4217	-.650441
102	4260	-.647994
103	4296	-.646390
104	4334	-.645153
105	4377	-.644390

Monte Carlo calculation of $\langle G(\bar{x}_1, \bar{x}_2) \rangle$, where

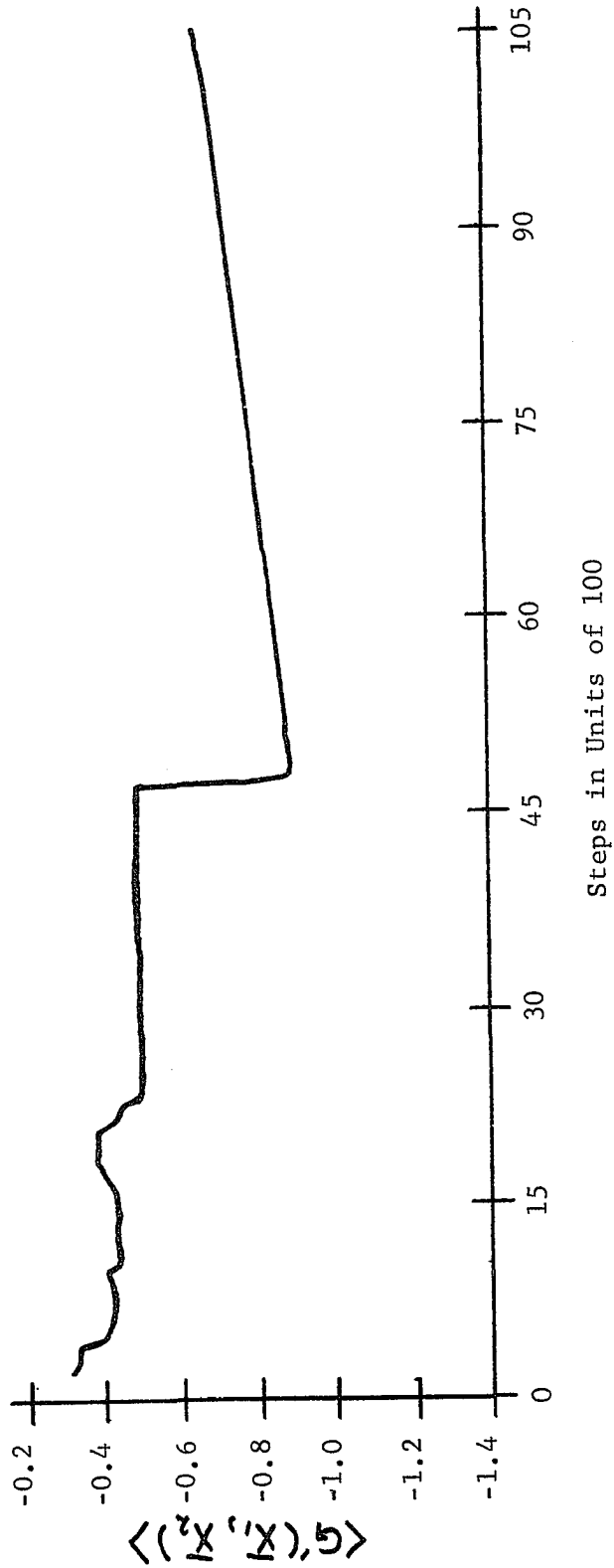
$$G(\bar{x}_1, \bar{x}_2) = \exp[|\bar{x}_1|^2 + |\bar{x}_2|^2 + |\bar{x}_1 - \bar{x}_2|^2] G_A(\bar{x}_1, \bar{x}_2).$$


Figure 5

CHAPTER IV

CONCLUSION

11 Evaluation of Results

The first thing we must note in this chapter is that each of the four attempts at evaluating $I_A(\pi/10)$ made in the last chapter would indeed give the correct value if enough computer time were used, thereby allowing enough points to be taken. In principle, then, we have solved the problem four times over, since we need allow only an infinite amount of time for each Monte Carlo process, in any of the "solutions" given, to obtain the correct result. It is clear, however, that this approach is quite impractical, and that we must be more critical in our evaluation.

The four solutions obtained in the last chapter, $(I_A(\pi/10) = -2.44, -1.82, -3.23, -3.89)$, are of the same order of magnitude. One might even say that they are quite close together, or at least that they are all uniformly inconclusive. How then can we say that one is better than another, or that we choose this approach or that as the one best suited for further use, such as the calculation of $P(\bar{\epsilon})$? The answer is really quite simple, and we have, indeed, already alluded to it.

The best function found is one used in section 10. The reason, as we mentioned in that section, is simply that both

$\int \dots \int F'(\bar{X}_1, \bar{X}_2) d\bar{X}_1 d\bar{X}_2$, and $P(\bar{X}_1, \bar{X}_2)$ are independent of the parameter $\bar{\ell}$, unlike the other solutions considered. Thus we can generate solutions for $I_A(\bar{\ell})$ for all values of $\bar{\ell}$ at once, with just one long Monte Carlo run, generating just one long series of steps for all $\langle G'(\bar{X}_1, \bar{X}_2, \bar{\ell}) \rangle$. With the other functions used we would have had to calculate each $I_A(\bar{\ell})$ separately, and each of these calculations would have had to have been as long as the one calculation suggested above. In addition we would have had to repeat the process for each $I_B(\bar{\ell})$, Eq. (7.2), before $F(\bar{\ell})$, and thus $P(\bar{\epsilon})$, could be known for all values of $\bar{\ell}$. With the functions used in section 10, however, neither the configuration of points, nor the normalizing constant of $P(\bar{X}_1, \bar{X}_2)$, depend on $\bar{\ell}$. Hence only two calculations are needed to generate all of the $I_A(\bar{\ell})$ and $I_B(\bar{\ell})$, and these calculations can be made very long and therefore very accurate, while still affording a great savings in time over the other functions considered. It should also be noted that the IBM 1620 computer required only about seven minutes per hundred points, with the function of section 10, as opposed to eight minutes for the fastest of the other functions, thereby giving it yet another advantage.

We feel, then, that the relative consistency of the four solutions to $I_A(\pi/10)$ given allows us to have some confidence that each of the methods would give the correct results. Hence we turn to the problem of actually calculating $P(\bar{\epsilon})$.

12 Suggestions for Further Study

The ultimate objective of research on this problem is the calculation of $P(\bar{\epsilon})$ for several values of the temperature-density parameter, Θ , and the particle size, σ , via the Kelbg theory. By comparison with the $P(\bar{\epsilon})$ calculated from the Holtmark theory, one could then determine at which values of Θ and σ the assumption that $U(\bar{r}_1, \dots, \bar{r}_N) = 0$ breaks down. Thus one could say that at a certain density and/or temperature the two component interaction term must be considered in the calculations.

One could then make a direct Monte Carlo calculation of Eq.(2.3),

$$P(\bar{\epsilon}) = \int \dots \int P(\bar{r}_1, \dots, \bar{r}_N) \delta(\bar{\epsilon} - \sum_{i=1}^N \bar{\epsilon}_i) d\bar{r}_1 \dots d\bar{r}_N,$$

where $P(\bar{r}_1, \dots, \bar{r}_N)$ is defined by Eq.(2.1), and, since this would presumably include all orders of particle interaction, one could tell at what density the interactions, higher than the second order, become important.

All of this can be accomplished by evaluating $F(\bar{l})$ for, perhaps ten or twenty particular values of \bar{l} , and these \bar{l} values can be determined by doing a Fourier analysis of the problem. We feel that methods outlined in this thesis, using the functions given in section 10 will make the calculations quite easy to do, given a fast enough computer. The IBM 1620, which was used in our work, is simply too slow for this task. For example the run which gave the values in Table VIII took over 750 minutes, and good convergence of the function is still not obtained. With

the IBM System/360 computer, however, this time will be cut by at least a factor of ten, thereby making the calculations quite practical.

APPENDICES

Appendix A

The Holtsmark Distribution

The probability distribution for finding an electric field of magnitude E at a given point in a classical system of N charged particles in thermodynamic equilibrium with absolute temperature T , is given by

$$P'(E) = 4\pi E^2 P(\bar{E})$$

$$= 4\pi E^2 \int \dots \int P(\bar{r}_1, \dots, \bar{r}_N) \delta(\bar{E} - \sum_{i=1}^N \bar{E}_i) \prod_{i=1}^N d\bar{r}_i, \quad (\text{A.1})$$

where

$$P(\bar{r}_1, \dots, \bar{r}_N) = \frac{\exp[-U(\bar{r}_1, \dots, \bar{r}_N)/k_0 T]}{\int \dots \int \exp[-U(\bar{r}_1, \dots, \bar{r}_N)/k_0 T] d\bar{r}_1 \dots d\bar{r}_N}. \quad (\text{A.2})$$

Here δ is the Dirac delta function, \bar{E}_i the electric field intensity from particle i at the point in question, \bar{E} the total electric field intensity at that point, k_0 is Boltzmann's constant, and $U(\bar{r}_1 \dots \bar{r}_N)$ is the total electrostatic potential energy of the system. Now the assumption made in the Holtsmark theory¹ is that there are no electrostatic particle interactions. Thus $U(\bar{r}_1 \dots \bar{r}_N) = 0$, and we have

$$P(\bar{E}) = \frac{1}{V^N} \int \dots \int \delta(\bar{E} - \sum_{i=1}^N \bar{E}_i) d\bar{r}_1 \dots d\bar{r}_N, \quad (\text{A.3})$$

since Eq.(A.2) becomes

$$P(\bar{r}_1, \dots, \bar{r}_N) = \frac{1}{\int \dots \int d\bar{r}_1 \dots d\bar{r}_N} = \frac{1}{V^N}$$

Now $P(\bar{E})$ is simply a function of \bar{E} , so we may write its Fourier

transform as

$$F(\bar{k}) = \iiint P(\bar{E}) \exp(i\bar{k} \cdot \bar{E}) d\bar{E}, \quad (\text{A.4})$$

so that

$$P(\bar{E}) = \frac{1}{(2\pi)^3} \iiint F(\bar{k}) \exp(-i\bar{k} \cdot \bar{E}) d\bar{k}. \quad (\text{A.5})$$

The reason for doing this is that Eq.(A.4) can be evaluated more easily than Eq.(A.3), and once $F(\bar{k})$ is known for all values of \bar{k} , Eq.(A.5) can be solved for $P(\bar{E})$.

To accomplish this we first write Eq.(A.4) as

$$F(\bar{k}) = \frac{1}{V^N} \int \cdots \int \delta(\bar{E} - \sum_{i=1}^N \bar{E}_i) \exp(i\bar{k} \cdot \bar{E}) \prod_{i=1}^N d\bar{r}_i d\bar{E}, \quad (\text{A.6})$$

and then we integrate over $d\bar{E}$ to get

$$\begin{aligned} F(\bar{k}) &= \frac{1}{V^N} \int \cdots \int \exp(i\bar{k} \cdot \sum_{i=1}^N \bar{E}_i) \prod_{i=1}^N d\bar{r}_i \\ &= \frac{1}{V^N} \prod_{i=1}^N \int \exp(i\bar{k} \cdot \bar{E}_i) d\bar{r}_i \\ &= \frac{1}{V^N} \left[\int \exp(i\bar{k} \cdot \bar{E}) d\bar{r} \right]^N. \end{aligned} \quad (\text{A.7})$$

This last form results since the N integrals are identical,

and hence the subscripts are not needed. We are now in a position

to go through a series of steps to evaluate this integral in

exact form, starting with

$$\begin{aligned} F(\bar{k}) &= \frac{1}{V^N} \left[\int (\exp(i\bar{k} \cdot \bar{E}) + 1 - 1) d\bar{r} \right]^N \\ &= \frac{1}{V^N} \left[\int d\bar{r} - \int (1 - \exp(i\bar{k} \cdot \bar{E})) d\bar{r} \right]^N \\ &= \left[1 - \frac{1}{N} \left(\frac{N}{V} \right) \int (1 - \exp(i\bar{k} \cdot \bar{E})) d\bar{r} \right]^N \end{aligned}$$

Now if N is large, and we shall assume that it is, we use the identity

$$\lim_{N \rightarrow \infty} \left[1 - \frac{x}{N}\right]^N = e^{-x}$$

to give

$$\begin{aligned} F(\bar{k}) &= \exp\left[-\frac{N}{V} \int (1 - \exp(i\bar{k} \cdot \bar{E})) d\bar{r}\right] \\ &= \exp\left[-\frac{N}{V} \int (1 - \exp(i\bar{k} \cdot \frac{\bar{r}}{r^3} c)) d\bar{r}\right], \end{aligned} \quad (\text{A.8})$$

where $\bar{E} = \frac{c\bar{r}}{r^3}$, and $c \equiv \frac{e}{4\pi\epsilon_0}$. Hence our problem is to solve the integral

$$I(\bar{k}) = \int (1 - \exp(i\frac{c}{r^3} \bar{k} \cdot \bar{r})) d\bar{r}. \quad (\text{A.9})$$

To do this we choose $\bar{k} = k\hat{e}_z$, i.e. \bar{k} points along the z -axis.

This gives

$$\begin{aligned} I(\bar{k}) &= \int_0^\infty \int_0^\pi \int_0^{2\pi} (1 - \exp[i\frac{(kc)\cos\theta}{r^2}]) r^2 \sin\theta dr d\theta d\varphi \\ &= 2\pi \int_0^\pi (1 - \exp[i\frac{(kc)\cos\theta}{r^2}]) r^2 \sin\theta dr d\theta, \end{aligned}$$

and if we let $U \equiv \cos\theta$, we have $dU = -\sin\theta d\theta$, resulting in

$$\begin{aligned} I(\bar{k}) &= -2\pi \int_1^{-1} \int_0^\infty (1 - \exp[i\frac{kcU}{r^2}]) du r^2 dr \\ &= 2\pi \int_0^\infty \left(U \Big|_{-1}^1 - \frac{r^2}{kc i} \exp[i\frac{kcU}{r^2}] \Big|_{-1}^1 \right) r^2 dr \quad (\text{A.10}') \\ &= 2\pi \int_0^\infty \left(1 + 1 - \frac{r^2}{kc i} (e^{i\frac{kc}{r^2}} - e^{-i\frac{kc}{r^2}}) \right) r^2 dr \\ &= 2\pi \int_0^\infty \left(2 - \frac{2r^2}{kc} \sin\left(\frac{kc}{r^2}\right) \right) r^2 dr. \quad (\text{A.10}) \end{aligned}$$

Now we let $t \equiv \frac{Kc}{r^2}$, so that $r^2 = \frac{Kc}{t}$, $dr = (-1/2)(Kc)^{1/2} t^{-3/2} dt$,
and $t \rightarrow \infty$ as $r \rightarrow 0$, thus

$$\begin{aligned} I(r) &= -2\pi \frac{1}{2} (Kc)^{3/2} 2 \int_0^{\infty} [1 - t^{-1} \sin t] t^{-5/2} dt \\ &= 2\pi (Kc)^{3/2} \int_0^{\infty} [t - \sin t] t^{-7/2} dt. \end{aligned} \quad (\text{A.11})$$

The integral in Eq.(A.11) can be solved exactly in the following way:

$$\begin{aligned} Q(t) &= \int_0^{\infty} t^{-5/2} dt - \int_0^{\infty} t^{-7/2} \sin t dt \\ &= -\frac{2}{3} t^{-3/2} - \int_0^{\infty} t^{-7/2} \sin t dt. \end{aligned}$$

Note that²⁴

$$(1) \int_0^{\infty} t^n \sin t dt = \frac{t^{n+1}}{n+1} \sin t \Big|_0^{\infty} - \frac{1}{n+1} \int_0^{\infty} t^{n+1} \cos t dt$$

$$(2) \int_0^{\infty} t^n \cos t dt = \frac{t^{n+1}}{n+1} \cos t \Big|_0^{\infty} + \frac{1}{n+1} \int_0^{\infty} t^{n+1} \sin t dt$$

$$(3) \int_0^{\infty} t^{-1/2} \cos t dt = \int_0^{\infty} t^{-1/2} \sin t dt = \sqrt{\frac{\pi}{2}}.$$

Thus we have (for $A \equiv (-2/3)t^{-3/2}$)

$$\begin{aligned} Q(t) &= A + \frac{t^{-5/2}}{(5/2)} \sin t \Big|_0^{\infty} - \frac{1}{(5/2)} \int_0^{\infty} t^{-5/2} \cos t dt \\ &= A + B + \frac{t^{-3/2}}{(5/2)(3/2)} \cos t \Big|_0^{\infty} + \frac{1}{(5/2)(3/2)} \int_0^{\infty} t^{-3/2} \sin t dt \\ &= A + B + C - \frac{t^{-1/2}}{(5/2 \cdot 3/2 \cdot 1/2)} \sin t \Big|_0^{\infty} + \frac{1}{(5/2 \cdot 3/2 \cdot 1/2)} \int_0^{\infty} t^{-1/2} \cos t dt \\ &= \left[-\left(\frac{2}{3}\right) t^{-3/2} + \left(\frac{2}{5}\right) t^{-5/2} \sin t + \left(\frac{4}{15}\right) t^{-3/2} \cos t \right. \\ &\quad \left. - \left(\frac{8}{15}\right) t^{-1/2} \sin t \right] \Big|_0^{\infty} + \frac{8}{15} \sqrt{\frac{\pi}{2}}. \end{aligned}$$

Now we can write

$$\begin{aligned}
Q(z) &= \lim_{\epsilon \rightarrow 0} \left[-\frac{2}{3}(-\epsilon^{-3/2}) + \frac{2}{5}(-\epsilon^{5/2} \sin \epsilon) + \frac{4}{15}(-\epsilon^{-3/2} \cos \epsilon) \right. \\
&\quad \left. - \frac{8}{15}(-\epsilon^{-1/2} \sin \epsilon) \right] + \frac{8}{15} \sqrt{\frac{\pi}{2}} \\
&= \lim_{\epsilon \rightarrow 0} \left[\left(\frac{2}{3} - \frac{2}{5} - \frac{4}{15} \right) \epsilon^{-3/2} + (\text{constant}) \epsilon^{1/2} \right. \\
&\quad \left. + (\text{constant}) \epsilon^{5/2} + \dots \right] + \frac{8}{15} \sqrt{\frac{\pi}{2}}.
\end{aligned}$$

Thus the above equation finally becomes

$$Q(z) = \frac{8}{15} \sqrt{\frac{\pi}{2}}. \quad (\text{A.12})$$

Substituting Eq. (A.12) into Eq. (A.11) gives

$$I(\bar{k}) = 2\pi (kc)^{3/2} \frac{8}{15} \sqrt{\frac{\pi}{2}},$$

and substituting this result into Eq. (A.8) yields

$$F(\bar{k}) = \exp\left[-\frac{N}{V} \frac{8\pi}{15} (kc)^{3/2} (2\pi)^{1/2}\right]. \quad (\text{A.13})$$

This is an exact solution to Eq. (A.4), and it may now be substituted into Eq. (A.5) to give

$$P(\bar{E}) = \frac{1}{(2\pi)^3} \int \exp[-Ak^{3/2}] \exp(i\bar{k} \cdot \bar{E}) d\bar{k},$$

where $A \equiv \frac{N}{V} \frac{8\pi}{15} c^{3/2} (2\pi)^{1/2}$. Using spherical coordinates we have

$$\begin{aligned}
P(\bar{E}) &= \frac{1}{(2\pi)^3} \int_0^{2\pi} \int_0^{\pi} \int_0^{\infty} e^{-Ak^{3/2}} e^{-ikE \cos \theta} k^2 \sin \theta dk d\theta d\phi \\
&= \frac{1}{(2\pi)^2} \int_0^{\pi} \int_0^{\infty} e^{-Ak^{3/2}} e^{-ikE \cos \theta} k^2 \sin \theta dk d\theta.
\end{aligned}$$

Now let $U = \cos \theta$, so $dU = -\sin \theta d\theta$, thereby giving the same result as in Eq. (A.10), i.e.

$$\begin{aligned}
 P(\bar{E}) &= \int_0^{\infty} (2\pi)^{-2} e^{-Ak^{3/2}} \frac{2}{kE} \sin(kE) k^2 dk \\
 &= \frac{2}{(2\pi)^2 E} \int_0^{\infty} \exp[-Ak^{3/2}] k \sin(kE) dk.
 \end{aligned}$$

If $x \equiv kE$, then $dk = \frac{1}{E} dx$, giving

$$P(\bar{E}) = \frac{2}{(2\pi)^2 E^3} \int_0^{\infty} \exp\left[-A\left(\frac{x}{E}\right)^{3/2}\right] x \sin x dx.$$

Define $\beta \equiv E/A^{2/3}$, so $A/E^{3/2} = 1/\beta^{3/2}$,

and therefore we have

$$\begin{aligned}
 P(\bar{E}) &= \frac{2}{(2\pi)^2 E^3} \int_0^{\infty} \exp\left[-\left(\frac{x}{\beta}\right)^{3/2}\right] x \sin x dx \\
 &= \frac{2}{(2\pi)^2 \beta^3 A^2} \int_0^{\infty} \exp\left[-\left(\frac{x}{\beta}\right)^{3/2}\right] x \sin x dx \\
 &= H(\beta) / 4\pi \beta^2 A^2. \tag{A.14}
 \end{aligned}$$

Here we have defined $H(\beta)$ as

$$H(\beta) \equiv \frac{2}{\pi \beta} \int_0^{\infty} \exp\left[-\left(\frac{x}{\beta}\right)^{3/2}\right] x \sin x dx, \tag{A.15}$$

and this function has been tabulated by S. Chandrasekhar¹ whose values are given in our Table (A-1).

We have thus arrived at the final result for the microfield distribution assuming no particle interactions, and we write it as

$$P'(\bar{E}) = 4\pi E^2 P(\bar{E}) = E^2 H(\beta) / \beta^2 A^2,$$

but

$$E^2 / \beta^2 A^2 = A^{-2/3}$$

so

$$P'(\bar{E}) = H(\beta) / A^{2/3}, \tag{A.16}$$

where $A \equiv \frac{N}{V} \frac{8\pi}{15} c^{3/2} (2\pi)^{1/2}$, (A.17)

and $C \equiv e / 4\pi \epsilon_0$. (A.18)

Notice that the Holtmark distribution is independent of the charge of the particles of the system. If they are all negative then $c = \frac{-e}{4\pi \epsilon_0}$, but $F(\vec{k})$ and $P(\vec{E})$ are unchanged, since a negative c can be put into Eq.(A.10') giving

$$\begin{aligned} I(k) &= 2\pi \int_0^\infty \left[U - \frac{r^2}{k(-c)i} \exp\left[i \frac{k(-c)U}{r^2}\right] \right] r^2 dr \\ &= 2\pi \int_0^\infty \left[1 + 1 + \frac{r^2}{ikc} \left(e^{-i \frac{kc}{r^2}} - e^{i \frac{kc}{r^2}} \right) \right] r^2 dr \\ &= 2\pi \int_0^\infty \left[2 - \frac{2r^2}{kc} \sin\left(\frac{kc}{r^2}\right) \right] r^2 dr. \end{aligned} \quad (\text{A.19})$$

Clearly Eq.(A.19) is the same as Eq.(A.10), so no matter what the sign of the charges in the system, $F(\vec{k})$ is as given by Eq.(A.13), with $c = \frac{+e}{4\pi \epsilon_0}$.

Table A-1. The Function $H(\beta) = \frac{2}{\pi\beta} \int_0^{\infty} \exp[-(\frac{x}{\beta})^{3/2}] x \sin x dx$.

β	$H(\beta)$	β	$H(\beta)$
0.0	0.000000	5.0	0.04310
0.1	0.004225	5.2	0.03790
0.2	0.016666	5.4	0.03357
0.3	0.036643	5.6	0.02993
0.4	0.063084	5.8	0.02683
0.5	0.094601	6.0	0.02417
0.6	0.129598	6.2	0.02188
0.7	0.166380	6.4	0.01988
0.8	0.203270	6.6	0.01814
0.9	0.238704	6.8	0.01660
1.0	0.271322	7.0	0.01525
1.1	0.30003	7.2	0.01405
1.2	0.32402	7.4	0.01297
1.3	0.34281	7.6	0.01201
1.4	0.35620	7.8	0.01115
1.5	0.36426	8.0	0.01038
1.6	0.36726	8.2	0.00967
1.7	0.36566	8.4	0.00903
1.8	0.36004	8.6	0.00846
1.9	0.35101	8.8	0.00793
2.0	0.33918	9.0	0.00745
2.1	0.32519	9.2	0.00701
2.2	0.30951	9.4	0.00660
2.3	0.29266	9.6	0.00622
2.4	0.27485	9.8	0.00588
2.5	0.25667	10.0	0.00556
2.6	0.238	15.0	0.00188
2.7	0.222	20.0	0.00089
2.8	0.206	25.0	0.00050
2.9	0.190	30.0	0.00031
3.0	0.176	35.0	0.00021
3.2	0.150	40.0	0.00015
3.4	0.128	45.0	0.00011
3.6		50.0	0.00009
3.8	These values are not	60.0	0.00005
4.0	given by Chandrasekhar.	70.0	0.00004
4.2		80.0	0.00003
4.4	0.06734	90.0	0.00002
4.6	0.05732	100.0	0.00002
4.8	0.04944		

APPENDIX B

The Kelbg Theory

As in Appendix A we write the electric distribution in the form

$$P(\bar{E}) = \int \dots \int P(\bar{r}_1, \dots, \bar{r}_N) \delta(\bar{E} - \sum_{i=1}^N \bar{E}_i) \prod_{i=1}^N d\bar{r}_i, \quad (\text{B.1})$$

where

$$P(\bar{r}_1, \dots, \bar{r}_N) = \frac{\exp[-U(\bar{r}_1, \dots, \bar{r}_N)/k_0 T]}{\int \dots \int \exp[-U(\bar{r}_1, \dots, \bar{r}_N)/k_0 T] \prod_{i=1}^N d\bar{r}_i}. \quad (\text{B.2})$$

However, in the Kelbg theory^{3,13} one does not assume that $U(\bar{r}_1 \dots \bar{r}_N) = 0$, i.e. particle interactions are not ignored. Thus, in order to solve Eq.(B.1), we again write the Fourier transform of $P(\bar{E})$, giving

$$\begin{aligned} F(\bar{k}) &= \iiint P(\bar{E}) \exp(i\bar{k} \cdot \bar{E}) d\bar{E} \\ &= \int \dots \int P(\bar{r}_1, \dots, \bar{r}_N) \exp(i\bar{k} \cdot \bar{E}) \delta(\bar{E} - \sum_{i=1}^N \bar{E}_i) \prod_{i=1}^N d\bar{r}_i d\bar{E}. \end{aligned}$$

Now we integrate over $d\bar{E}$. Hence

$$F(\bar{k}) = \int \dots \int P(\bar{r}_1, \dots, \bar{r}_N) \prod_{i=1}^N \exp(i\bar{k} \cdot \bar{E}_i) d\bar{r}_i. \quad (\text{B.3})$$

Define

$$\Omega_i \equiv \exp(i\bar{k} \cdot \bar{E}_i),$$

and

$$\omega_i \equiv \int \Omega_i P_i(\bar{r}_i) d\bar{r}_i.$$

Note that

$$P_i(\bar{r}_i) \equiv \frac{\int \dots \int e^{-U/k_0 T} d\bar{r}_1 \dots d\bar{r}_{i-1} d\bar{r}_{i+1} \dots d\bar{r}_N}{\int \dots \int e^{-U/k_0 T} d\bar{r}_1 \dots d\bar{r}_N}.$$

Now write the identity

$$\Omega_i = \omega_i \left[1 + \left(\frac{\Omega_i}{\omega_i} - 1 \right) \right],$$

and substitute this into Eq. (B.3). This gives

$$\begin{aligned} F(\bar{r}) &= \int \dots \int P(\bar{r}_1, \dots, \bar{r}_N) \prod_{i=1}^N \Omega_i d\bar{r}_i \\ &= \int \dots \int P(\bar{r}_1, \dots, \bar{r}_N) \prod_{i=1}^N \omega_i \left[1 + \left(\frac{\Omega_i}{\omega_i} - 1 \right) \right] d\bar{r}_i. \end{aligned} \quad (\text{B.4})$$

Now

$$\begin{aligned} \prod_{i=1}^N \omega_i \left[1 + \left(\frac{\Omega_i}{\omega_i} - 1 \right) \right] &= \omega_1 \dots \omega_N \prod_{i=1}^N \left[1 + \left(\frac{\Omega_i}{\omega_i} - 1 \right) \right] \\ &= \prod_{i=1}^N \omega_i \left[1 + \sum_{i=1}^N \left(\frac{\Omega_i}{\omega_i} - 1 \right) + \frac{1}{2} \sum_{i < j=1}^N \left(\frac{\Omega_i \Omega_j}{\omega_i \omega_j} - \frac{\Omega_i}{\omega_i} - \frac{\Omega_j}{\omega_j} + 1 \right) + \dots \right] \\ &= \prod_{i=1}^N \omega_i \left[1 + \sum_{i=1}^N \left(\frac{\Omega_i}{\omega_i} - 1 \right) + \frac{1}{2} \sum_{i < j=1}^N \left(\frac{\Omega_i \Omega_j}{\omega_i \omega_j} - \left[\frac{\Omega_i}{\omega_i} - 1 \right] - \left[\frac{\Omega_j}{\omega_j} - 1 \right] - 1 \right) + \dots \right]. \end{aligned}$$

Thus Eq. (B.4) becomes

$$F(\bar{r}) = \int \dots \int P(\bar{r}_1, \dots, \bar{r}_N) \prod_{i=1}^N \omega_i \left[1 + \sum_{i=1}^N \left(\frac{\Omega_i}{\omega_i} - 1 \right) + \dots \right] d\bar{r}_i. \quad (\text{B.5})$$

Now the second term in the sum above will vanish as we shall now show. To do this we write

$$\begin{aligned} & \int \dots \int P(\bar{r}_1, \dots, \bar{r}_N) \left(\frac{\Omega_i}{\omega_i} - 1 \right) d\bar{r}_1 \dots d\bar{r}_N \\ &= \frac{\int \dots \int e^{-U/k_0 T} \left(\frac{\Omega_i}{\omega_i} - 1 \right) d\bar{r}_1 \dots d\bar{r}_N}{\int \dots \int e^{-U/k_0 T} d\bar{r}_1 \dots d\bar{r}_N} \\ &= \frac{\int \dots \int e^{-U/k_0 T} \left(\frac{\Omega_i}{\omega_i} \right) d\bar{r}_1 \dots d\bar{r}_N}{\int \dots \int e^{-U/k_0 T} d\bar{r}_1 \dots d\bar{r}_N} - 1 \\ &= \frac{1}{\omega_i} \left[\int \Omega_i P_i(\bar{r}_i) d\bar{r}_i - \omega_i \right] \end{aligned}$$

$$= \frac{1}{\omega_i} [\omega_i - \omega_i]$$

$$= 0.$$

Thus Eq. (B.5) becomes

$$F(\bar{k}) = \int \dots \int P(\bar{r}_1, \dots, \bar{r}_N) \prod_{i=1}^N \omega_i \left[1 + \frac{1}{2} \sum_{i < j=1}^N \left(\frac{\Omega_i \Omega_j}{\omega_i \omega_j} - 1 \right) + \dots \right] d\bar{r}_i$$

$$= \prod_{i=1}^N \omega_i \left[1 + \frac{1}{2} \sum_{i < j=1}^N \int \dots \int P(\bar{r}_1, \dots, \bar{r}_N) \left(\frac{\Omega_i \Omega_j}{\omega_i \omega_j} - 1 \right) d\bar{r}_1 \dots d\bar{r}_N + \dots \right] \quad (\text{B.6})$$

This last equation results since the ω_i are not functions of the \bar{r}_i , and

$$\int \dots \int P(\bar{r}_1, \dots, \bar{r}_N) d\bar{r}_1 \dots d\bar{r}_N = 1.$$

Hence we may divide $F(\bar{k})$ into two components

$$F(\bar{k}) = F_0(\bar{k}) F_1(\bar{k}),$$

where

$$F_0(\bar{k}) \equiv \prod_{i=1}^N \omega_i,$$

and $F_1(\bar{k})$ equals the remaining series of terms. Note that so far the derivation has been exact, and that we have simply used definitions and identities to change the form of the original form of the equation, Eq. (B.3), into that of Eq. (B.6).

It can now be shown that $F_0(\bar{k})$ as defined above is simply the Holtmark term. Hence we write

$$F_0(\bar{k}) \equiv \prod_{i=1}^N \omega_i \equiv \prod_{i=1}^N \int \Omega_i P_i(\bar{r}_i) d\bar{r}_i$$

$$= \prod_{i=1}^N \int \exp(i\bar{k} \cdot \bar{E}_i) P_i(\bar{r}_i) d\bar{r}_i$$

$$\begin{aligned}
&= \prod_{i=1}^N \frac{\int \dots \int \exp(i\bar{k} \cdot \bar{E}_i) \exp(-U/k_0 T) d\bar{r}_1 \dots d\bar{r}_N}{\int \dots \int \exp(-U/k_0 T) d\bar{r}_1 \dots d\bar{r}_N} \\
&= \prod_{i=1}^N \frac{\int \left[\int \dots \int \exp(-U/k_0 T) \prod_{j \neq i}^N d\bar{r}_j \right] \exp(i\bar{k} \cdot \bar{E}_i) d\bar{r}_i}{\int \dots \int \exp(-U/k_0 T) d\bar{r}_1 \dots d\bar{r}_N}. \quad (\text{B.7})
\end{aligned}$$

At this point we make the requirement that the field point at which $P(\bar{E})$ is to be calculated is a neutral point. Note also that we may write $P_1(\bar{r}_j)$ in terms of the correlation function g_1 , as shown earlier, resulting in

$$g_1(\bar{r}_i) = V \left\{ \frac{\int \dots \int \exp(-U/k_0 T) \prod_{j \neq i}^N d\bar{r}_j}{\int \dots \int \exp(-U/k_0 T) d\bar{r}_1 \dots d\bar{r}_N} \right\}. \quad (\text{B.8})$$

But, at a neutral point, the functions $g_1(\bar{r}_i)$ are equal to unity so the term in the bracket must equal $1/V$, and Eq. (B.7) becomes

$$\begin{aligned}
F_0(\bar{k}) &= \prod_{i=1}^N \frac{1}{V} \int \exp(i\bar{k} \cdot \bar{E}_i) d\bar{r}_i \\
&= \frac{1}{V^N} \left[\int \exp(i\bar{k} \cdot \bar{E}) d\bar{r} \right]^N. \quad (\text{B.9})
\end{aligned}$$

This is identical to Eq. (A.7) which is the Fourier transform of the Holtmark distribution. Thus we have shown that $F(\bar{k})$ in the Kelbg theory is just the Holtmark distribution multiplied by a series of correction terms of increasing particle correlation. Clearly then we may write $F_0(\bar{k})$ as

$$F_0(\bar{k}) = \exp \left[-\frac{N}{V} \int (1 - \exp(i\bar{k} \cdot \bar{E})) d\bar{r} \right] \quad (\text{B.10})$$

by following the same steps which took us from Eq. (A.7) to Eq. (A.8).

Now Kelbg simply generalizes Eq. (B.10) for the case of a system of "S" different types of particles, each having a number density

given by $n_j = N_j/V$, where there are N_j particles of type "j" in the system. Hence Eq. (B.10) becomes

$$F_0(\bar{k}) = \exp \left[\sum_{\sigma=1}^s n_{\sigma} \int (\Omega_{\sigma} - 1) d\bar{r}_{\sigma} \right], \quad (\text{B.11})$$

where σ labels the type of particles in this s -component system.

We now turn to $F_1(\bar{k})$, and it is here that Kelbg makes his one approximation. By assuming that the system is sufficiently tenuous, one could argue that the three-body, and higher correlation terms, are very small, since the chances of three, or more particles "getting together" are similarly small. By making this assumption, then, one can terminate the series in Eq. (B.6) after the second term. We may think of this truncated series as the "linearized" exponential series,

$$\begin{aligned} e^x &\equiv 1 + x + \frac{1}{2!} x^2 + \dots \\ &\approx 1 + x \quad (\text{for small } x), \end{aligned}$$

thereby allowing us to write

$$\begin{aligned} F_1(\bar{k}) &= \left[1 + \frac{1}{2} \sum_{i < j=1}^N \iint \left(\frac{\Omega_i \Omega_j}{\omega_i \omega_j} - 1 \right) P_2(\bar{r}_i, \bar{r}_j) d\bar{r}_i d\bar{r}_j + \dots \right] \\ &\approx \left[1 + \frac{1}{2} \sum_{i < j=1}^N \iint \left(\frac{\Omega_i \Omega_j}{\omega_i \omega_j} - 1 \right) P_2(\bar{r}_i, \bar{r}_j) d\bar{r}_i d\bar{r}_j \right] \\ &= \left[1 + \frac{N(N-1)}{2V^2} \iint \left(\frac{\Omega_1 \Omega_2}{\omega_1 \omega_2} - 1 \right) g_2(\bar{r}_1, \bar{r}_2) d\bar{r}_1 d\bar{r}_2 \right] \\ &\approx \exp \left[\frac{N(N-1)}{2V^2} \iint \left(\frac{\Omega_1 \Omega_2}{\omega_1 \omega_2} - 1 \right) g_2 d\bar{r}_1 d\bar{r}_2 \right]. \quad (\text{B.12}) \end{aligned}$$

Again we can generalize Eq. (B.12) for an S -component system,

but now we are concerned with two-particle interactions, so

the generalization must include summations over all possible combinations. This, then, results in

$$F_1(\bar{k}) = \exp \left[\frac{1}{2} \sum_{\sigma=1}^s \sum_{\tau=1}^s n_{\sigma} n_{\tau} \iint \left(\frac{\Omega_{\sigma} \Omega_{\tau}}{\omega_{\sigma} \omega_{\tau}} - 1 \right) g_2 d\bar{r}_{\sigma} d\bar{r}_{\tau} \right], \quad (\text{B.13})$$

where n_{σ} and n_{τ} are the particle densities of the two types of particles considered at any one time.

APPENDIX C

The Monte Carlo Method

The "Monte Carlo" technique¹⁸⁻²¹ for evaluating integrals numerically will be explained in this appendix. Presenting a rigorous proof of its validity is not our goal, but the interested reader may refer to the references given for such a proof. We shall instead present an "operational" description of the method, along with an example, using an integral which can be solved analytically, for verification.

We may write a general integral, then, as

$$I = \int_A^B F(x) G(x) dx, \quad (C.1)$$

where $F(x) G(x)$ can be any combination of specific functions, say $e^{-|x|} \cos x$. The next step is to normalize one of these functions, say $F(x)$, by writing

$$P(x) = \frac{F(x)}{\int_A^B F(x) dx},$$

so that

$$\int_A^B P(x) dx = 1.$$

Now we have

$$\begin{aligned} I &= \left\{ \int_A^B F(x) dx \right\} \int_A^B P(x) G(x) dx \\ &= \int_A^B F(x) dx \langle G(x) \rangle, \end{aligned} \quad (C.2)$$

where $\langle G(x) \rangle$ is the weighted average value of $G(x)$ in the range $A \leq x \leq B$, since $P(x)$ has become a normalized probability

distribution of points within this range. Note that $I(x)$ is unchanged by all of this, since we have merely multiplied and divided Eq.(C.1) by a constant, $\int_A^B F(x) dx$.

As an example let us write

$$I = \int_{-\infty}^{\infty} e^{-|x|} \cos x dx .$$

Now this can be solved analytically as follows:

$$\begin{aligned} I &= 2 \int_0^{\infty} e^{-x} \cos x dx \\ &= \frac{2}{2} e^{-x} (-\cos x + \sin x) \Big|_0^{\infty} = 1, \end{aligned}$$

which will serve as a check on our results. If we let $F(x) \equiv e^{-|x|}$ and $G(x) \equiv \cos x$, with $A = -\infty$ and $B = +\infty$, we have

$$\begin{aligned} \int_A^B F(x) dx &= \int_{-\infty}^{\infty} e^{-|x|} dx \\ &= 2 \int_0^{\infty} e^{-x} dx \\ &= -2 e^{-x} \Big|_0^{\infty} \\ &= 2 . \end{aligned}$$

Hence

$$P(x) = \frac{1}{2} e^{-|x|},$$

and

$$I = 2 \int_{-\infty}^{\infty} \left(\frac{1}{2} e^{-|x|} \right) \cos x dx . \quad (C.3)$$

This example points out one very important problem. That is, our ability to write Eq.(C.2) depends on our ability to evaluate $\int_A^B F(x) dx$. Clearly this may not always be possible, for we might have some $F(x)$ which is itself just as difficult to integrate as was $F(x) G(x)$. Thus we are faced with the possibility that the

functions may have been altered, say by substituting $F'(x) = H(x) F(x)$, and $G'(x) = H^{-1}(x) G(x)$, where $H(x) H^{-1}(x) = 1$, in the integral.

We then would have

$$\begin{aligned} I &= \int_A^B (H(x) F(x)) H^{-1}(x) G(x) dx \\ &= \left\{ \int_A^B H(x) F(x) dx \right\} \langle H^{-1}(x) G(x) \rangle \end{aligned}$$

in accordance with the substitutions made.

If the integral can be put in the form of Eq.(C.2), with $\int_A^B F(x) dx$ evaluated, then it can be solved using a computer. The method is similar to any other quadrature technique (Simpson's Rule, etc.), except that the points at which $G(x)$ is evaluated are picked under control of the probability function $P(x)$. Hence more points are concentrated in those regions of space where the integrand is large than in those where the integrand is small. This enables one to use a given number of points more efficiently than is possible with the other quadrature methods.

The points at which $G(x)$ is to be evaluated are chosen by selecting an arbitrary starting point (in this case any point on the x-axis). A second point is chosen by adding a random number between -1 and +1, multiplied by a fixed "step length", to the original coordinate position. Then $P_1(x)$ and $P_2(x)$, (where $P_1(x)$ is just $P(x)$ at the original point while $P_2(x)$ is $P(x)$ at the new point) are compared. If P_2 is greater than P_1 then $G(x)$ is evaluated at the new point. If P_2 is less than P_1 then P_2/P_1

is compared with a random number between 0 and 1. If P_2/P_1 is greater than a random number then $G(x)$ is evaluated at the new point; if, however, P_2/P_1 is less than a random number then $G(x)$ is evaluated at the old point. Once $G(x)$ is evaluated, it is added to a storage area so that $\langle G(x) \rangle$ may be finally calculated after a sufficient number of steps have been taken. The process is then repeated as many times as desired with the new starting position being either the previous old or new position depending upon whether $G(x)$ was evaluated at the old or new point. Figure (C.1) gives a block diagram of this process, and Table (C.I) gives the computer program used to evaluate

$$I = \int_{-\infty}^{\infty} e^{-|x|} \cos x \, dx .$$

Figure (C.2) gives the results of this calculation for increasing numbers of points, and these values should be compared with the analytical answer $I(x) = 1$.

Notice that in applying this method there are a few adjustable parameters which the investigator must cope with. Among these is the "step length", L , used to move to a new point. In making these random moves we write

$$X_{\text{new}} = X_{\text{old}} + 2L(\text{random number} - .5),$$

where the random number is generated by the IBM-1620 RANDF function and is between 0 and 1. Thus X_{new} is equal to X_{old} plus a random number between -1 and +1 multiplied by L . If L is too small not enough of the space will be explored with a given number of moves, and if L is too large $P_2(x)$ may be smaller than $P_1(x)$

Block Diagram of the computer program
used to make a Monte Carlo calculation

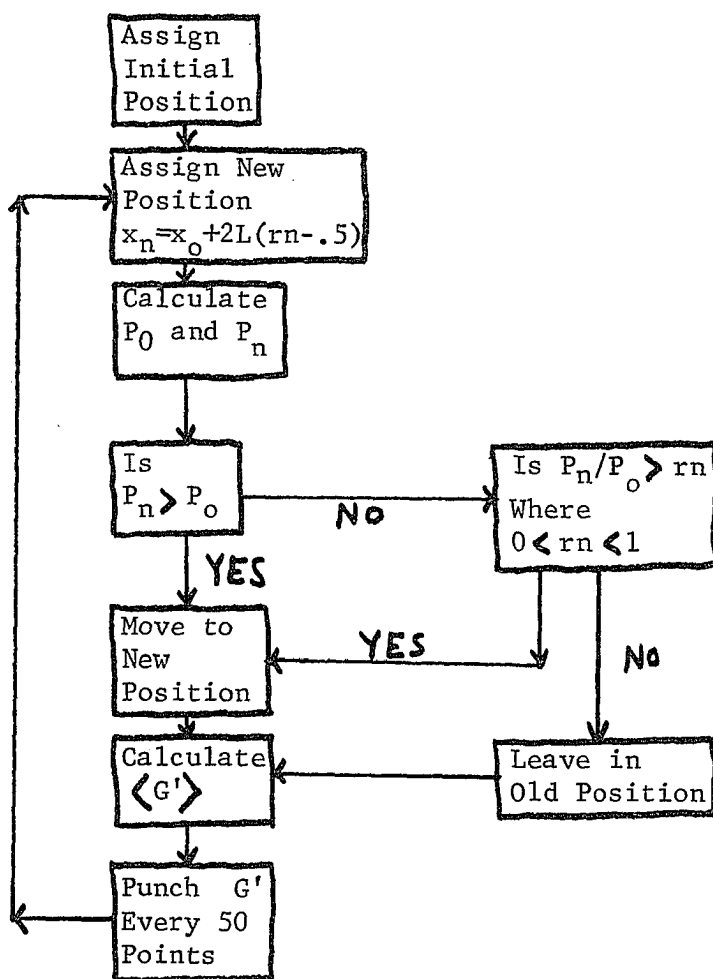


Figure C.1

Table C.I. Fortran IV program for the
Monte Carlo evaluation of the integral

$$\int_{-\infty}^{\infty} e^{-|x|} \cos x \, dx .$$

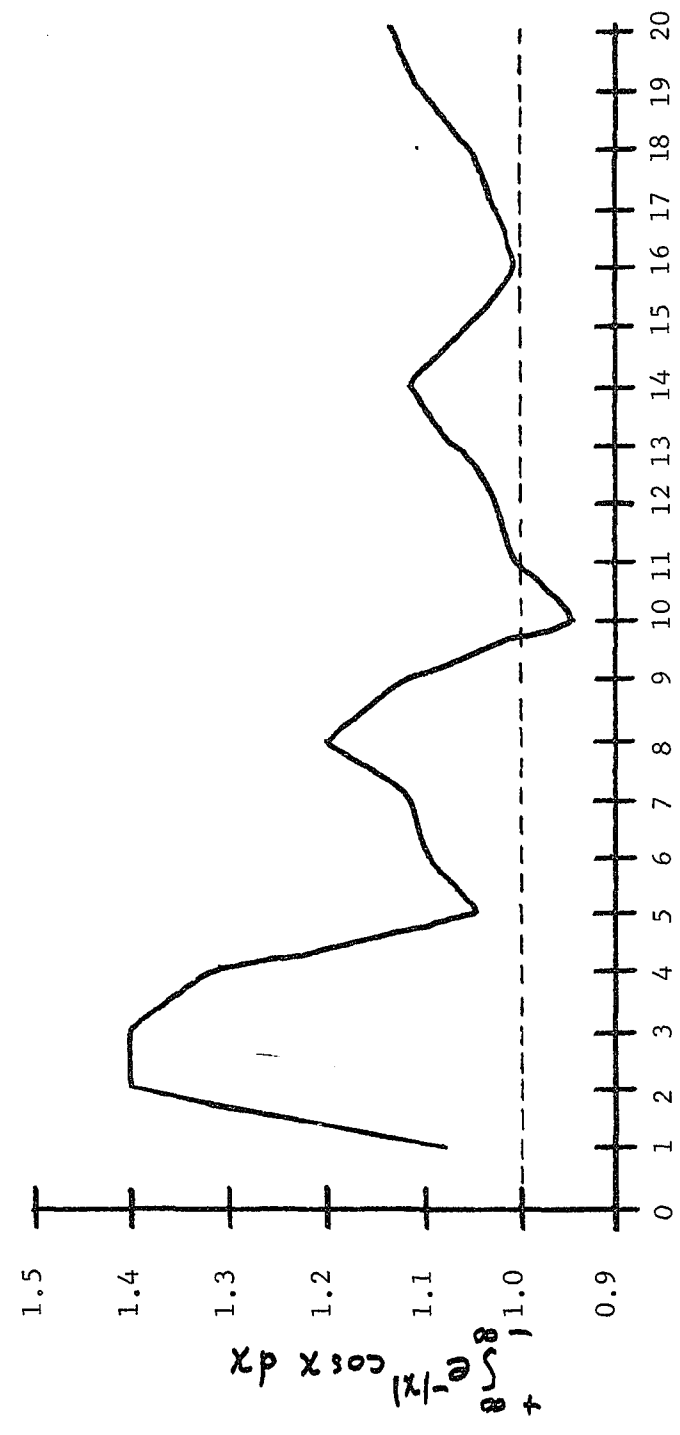
```

1  FORMAT(F10.6,4XF10.6,4X12)
   XOSIN=0.0000000
   XO=0.0000000
   DO 100 I=1,20
   DO 101 J=1,50
   RN=RANDF(.337)
   DEL=(RN-.5)*2.
   XN=XO + .5*DEL
   PROBO=EXPF(-ABS(XO))
   PROBN=EXPF(-ABS(XN))
   IF(PROBN-PROBO) 11,10,10
11  RN=RANDF(.337)
   IF(PROBN/PROBO-RN) 12,10,10
10  X=XN
   GO TO 13
12  X=XO
13  XOSIN=XOSIN+COSF(X)
101 XO=X
   XI=I
   VALUE=(XOSIN/XI*50.)*2.
100 PUNCH 1, VALUE,XO,I
   CALL EXIT
   END

```

A Monte Carlo calculation of the integral

$$\int_{-\infty}^{\infty} e^{-|x|} \cos x \, dx$$



Steps in Units of 50

Figure C.2

too many times, thereby preventing our evaluation point from moving enough, which also prevents our exploring enough of the space.

Another adjustable parameter is the starting point, which if poorly chosen could put the evaluation point in such a region as to make exploration of the entire space more time consuming than need be.

Finally note that if we have a $G(x)$ that is slowly varying the numerical evaluation of $\langle G(x) \rangle$ will be much easier than if $G(x)$ is wildly varying. Thus for a particular "bad" $G(x)$ the substitutions

$$F'(x) = H(x) F(x),$$

and

$$G'(x) = H^{-1}(x) G(x)$$

may have to be made so that $G'(x)$ is as slowly varying as possible, while $\int_A^B F'(x) dx$ is still solvable.

In this appendix we have considered only one-dimensional integrals. Clearly the Monte Carlo method is not limited to this case. In fact it is at its best when applied to multi-dimensional integrals, such as those encountered in this thesis.

Appendix D

The Simpson's Rule Calculation

The so-called Simpson's rule for evaluating an integral, is given by²³

$$\int_a^b f(x) dx \approx \frac{h}{3} (y_0 + 4y_1 + 2y_2 + 4y_3 + 2y_4 + \dots + 4y_{n-1} + y_n).$$

Here the interval $a < x < b$ is divided into an even number of subintervals, n , of length $h = (b-a)/n$. Then $y_0 = f(a)$, $y_1 = f(a+h)$, \dots , $y_{n-1} = f(b-h)$, $y_n = f(b)$.

The integral we consider here is given by Eq.(8.4), and we write it here

$$\int_0^{\infty} r^4 e^{-r^2} \sin\left[\frac{\ell}{r^2}\right] dr.$$

The integrand becomes very small for r greater than five, for at $r = 5$

$$\begin{aligned} r^4 e^{-r^2} &= 625 \times 25 \times 10^{-9} \times 6.74 \times 10^{-3} \\ &= 1.05 \times 10^{-7} \end{aligned}$$

Thus we integrated over the interval $0.01 \leq r \leq 5.71$ in 570 steps of length 0.01. The computer program, and its result, for $\ell = (\pi/10)$, are listed in Table (D.I). The program is written in the Fortran IV language for the IBM 1620 computer. The run time for this program was about eight minutes.

Table D.I. Fortran IV program for the
Simpson's Rule evaluation of

$$I(\ell) = \int_0^{\infty} r^4 e^{-r^2} \sin\left[\frac{\ell r}{r_1}\right] dr,$$

for $\ell = \pi/10$.

```

2 FORMAT (F10.7)
XL=3.1415926/10.
X=0.01
ADD=(X**4)*EXPF(-X**2)*SINF(XL/(X**2))
RESULT=(.01*ADD)/3.
DO 101 J=1,248
X=X+.01
ADD=(X**4)*EXPF(-X**2)*SINF(XL/(X**2))
RESULT=RESULT+((.04*ADD)/3.)
X=X+.01
ADD=(X**4)*EXPF(-X**2)*SINF(XL/(X**2))
101 RESULT=RESULT+((.02*ADD)/3.)
X=X+.01
ADD=(X**4)*EXPF(-X**2)*SINF(XL/(X**2))
RESULT=RESULT+((.04*ADD)/3.)
X=X+.01
ADD=(X**4)*EXPF(-X**2)*SINF(XL/(X**2))
RESULT=RESULT+((.01*ADD)/3.)
PUNCH 2, RESULT
CALL EXIT
END

```

RESULT = 0.1283

An identical program, for the evaluation of Eq.(9.1) was also written. The only change from that given in Table (D.I) was that the range extended to 7.03 instead of 5.71, and, of course, an r^6 replaced the r^4 of Eq.(8.4).

Appendix E

The Monte Carlo Computer Program for the Kelbg Integrals

In this appendix we give a listing of the Fortran IV computer program used in evaluating $\langle G'(\bar{X}_1, \bar{X}_2, (\pi/10)) \rangle$ in section 10 of this thesis. This program is identical to those used in all of the work presented in Chapter III, except for the changes in $P(\bar{X}_1, \bar{X}_2)$ and $G'(\bar{X}_1, \bar{X}_2)$ indicated in that chapter.

A block diagram of the program is given in Figure (E.1), and the program is listed in Table (E.I), where the numbered sections correspond to the blocks in the block diagram. Note that the block diagram includes only the major steps in the process, while the program itself has many details not indicated in Figure (E.1), some of which we shall now discuss.

First note that the program begins by reading in a table of values of g_A for particle separations from .05a to 7.4a, in the intervals of .05a. These values are called by the subscripted variable $G(I)$ in the program. Note also that in step 160 we write GV (defined as $g_A - 1$) equals 0.0 if the particle separation is greater than 7.4a. This is because $g_A - 1$ approaches zero very rapidly for particle separations as small as 2.0, which can be seen in Figure 2 of this thesis. Finally observe that in the Fortran statement immediately preceding statement number 16, we have calculated GV by a linear interpolation of the tabulated values whenever the particle separation (SEP) falls between two

tabulated values.



Block Diagram of the computer program
used to make a Monte Carlo calculation

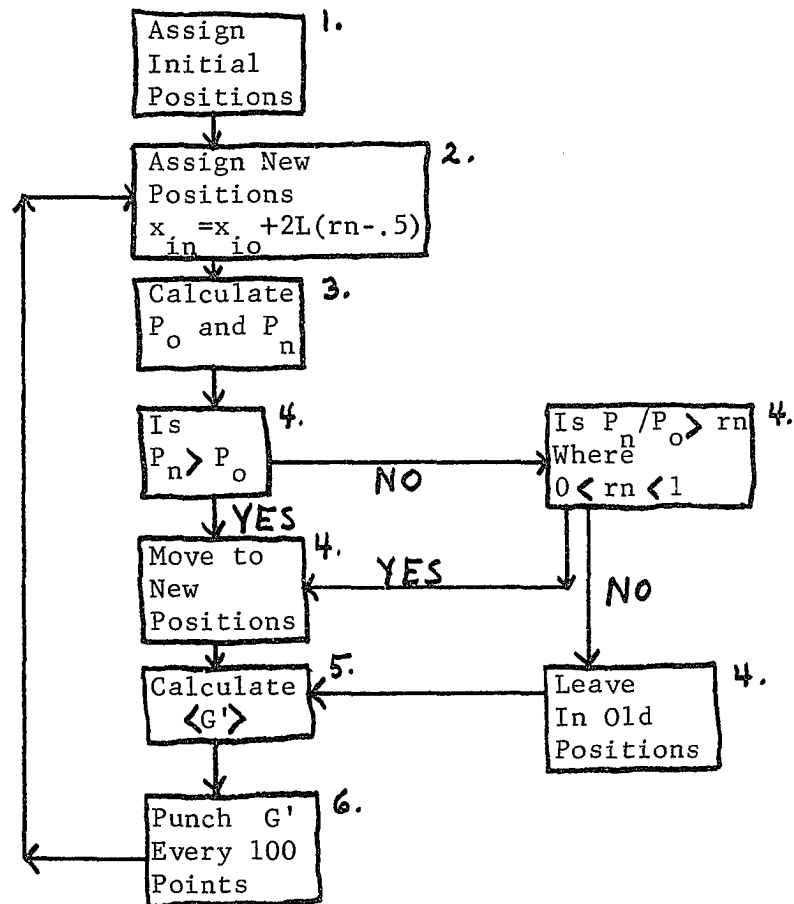


Figure E.1

Table E.I. Fortran IV program for the Monte Carlo evaluation of the integral

$$\int \dots \int [1 - \cos(R)] G_A(\bar{X}_1, \bar{X}_2) d\bar{X}_1 d\bar{X}_2 \cdot$$

```

      DIMENSION G(200)
      1 FORMAT(F10.6,1X14,1XF10.6,F10.6,F10.6,F10.6,F10.6,F10.6)
      2 FORMAT(I4,2XI4)
      3 FORMAT(4(1XE14.8))
      4 FORMAT(F9.8)
      READ 4, XL
      10 READ 3, (G(I), I=1,148)
1.      X1=.533946
         X2=-.009074
         Y1=-.654167
         Y2=-.985409
         Z1=-.024385
         Z2=.406052
         VALUE=0.000000
         NOMOV=0000
         DO 100, I=1,9999
         DO 101, J=1,100
2.      X1N=X1+(RANDF(.159)-.5)*.8
         X2N=X2+(RANDF(.159)-.5)*.8
         Y1N=Y1+(RANDF(.159)-.5)*.8
         Y2N=Y2+(RANDF(.159)-.5)*.8
         Z1N=Z1+(RANDF(.159)-.5)*.8
         Z2N=Z2+(RANDF(.159)-.5)*.8
3.      PO=EXPF(-2.*(X1**2+Y1**2+Z1**2+X2**2+Y2**2+Z2**2
         -X1*X2-Y1*Y2-Z1*Z2))
         PN=EXPF(-2.*(X1N**2+Y1N**2+Z1N**2+X2N**2+Y2N**2
         +Z2N**2-X1N*X2N-Y1N*Y2N-Z1N*Z2N))
4.      IF (PN-PO) 11,12,12
         11 IF (PN/PO-RANDF(.159)) 22,12,12
         22 NOMOV=NOMOV+1
         GO TO 13
         12 X1=X1N
            X2=X2N
            Y1=Y1N
            Y2=Y2N
            Z1=Z1N
            Z2=Z2N
5.      13 SEP=SQRTF((X1-X2)**2+(Y1-Y2)**2+(Z1-Z2)**2)
         IF (SEP-7.4) 150,160,160
         150 IF (SEP-.4) 170,151,151
         160 GV=0.0
         GO TO 101

```

Table E.1 continued

```

170 GV=-1.0
    GO TO 16
151 XK=(SEP/.05)
    K=XK+1.
    XK=K
    GV=G(K-1)+((SEP-.05*(XK-1.))* (G(K)-G(K-1))/.05)-1.
16  A=Z1/((X1**2+Y1**2+Z1**2)*SQRTF(X1**2+Y1**2+Z1**2))
    B=Z2/((X2**2+Y2**2+Z2**2)*SQRTF(X2**2+Y2**2+Z2**2))
    COA=XI*(A+B)
    EO=EXPF(2.*(X1**2+Y1**2+Z1**2+X2**2+Y2**2+Z2**2-X1*X2
        -Y1*Y2-Z1*Z2))
    VALUE=VALUE+(1.-COSF(COA))*EO*GV


---


6.  101 CONTINUE
    XI=I
    RESULT=VALUE/(XI*100.)
    PUNCH 1, RESULT,I,X1,X2,Y1,Y2,Z1,Z2
    PUNCH 2, NOMOV,I


---


100 CONTINUE
    CALL EXIT
    END

```

REFERENCES

1. Wax, Nelson (Ed.), Selected Papers on Noise and Stochastic Processes. New York: Dover Publications, Inc., 1954.
"Stochastic Problems in Physics and Astronomy,"
S. Chandrasekhar. Chapter 4, Sections 1 and 2, Pp. 70-76.
2. Broyles, A. A., Phys. Rev. 100, 1181 (1955) and 105, 347 (1957); Z. Physik 151, 187 (1958); AEC Report RM-1682, (Unpublished).
3. Conway, B. E. and Barradas, R. G. (Ed.), Chemical Physics of Ionic Solutions. New York: John Wiley and Sons, Inc., 1966. "Extensions of the Debye-Huckel Limiting Law; Applications to Ionic Solutions and Plasmas," G. Kelbg. Chapter 4, Pp. 48-52.
4. Lewis, M. and Margenau, H., Phys. Rev. 109, 842 (1958).
5. Edmonds, F. N., Astrophys. J. 123, 95 (1956).
6. Ecker, G., Z. Physik 148, 593 (1957).
7. Ecker, G. and Muller, K. G., Z. Physik 153, 317 (1958).
8. Hoffman, H. and Theimer, O., Astrophys. J. 127, 477 (1958).
9. Mayer, H., Los Alamos Scientific Laboratory, Report LA-647, 1947 (Unpublished).
10. Hooper, C. F. Jr., Phys. Rev. 149, 77 (1966).
11. Mozer, B., Thesis, Carnegie Institute of Technology (Unpublished). Chapter 4, Pp. 82-103. (1960).
12. Baranger, M. and Mozer, B., Phys. Rev. 115, 521 (1959) and 118, 626 (1960).
13. Kelbg, G., Ann. Physik 13, 385 (1964) and 14, 394 (1964).
14. Pines, D. and Bohm, D., Phys. Rev. 82, 625 (1951) and 85, 338 (1952).
15. Hill, T. L., Introduction to Statistical Thermodynamics. Reading, Mass.: Addison-Wesley Publishing Company, Inc., 1960. Chapter 17.

16. Debye, P. and Huckel, E., *Physik. Z.* 24, 185 (1923).
17. Carley, D. D., *J. Chem. Phys.* 46, 3783 (1967).
18. Metropolis, Rosenbluth, Rosenbluth, Teller, and Teller, *J. Chem. Phys.* 21, 1087 (1953).
19. Wood and Parker, *J. Chem. Phys.* 27, 720 (1957).
20. Bharucha and Reid, Elements of the Theory of Markov Processes and Their Applications. New York: McGraw-Hill Book Company, Inc., 1960.
21. Meyer, Herbert A. (Ed.), Symposium on Monte Carlo Methods. New York: John Wiley and Sons, Inc., 1956. "Generation and Testing of Pseudo-Random Numbers," O. Taussky and J. Todd. Pp. 15-28.
22. Mathews, Jon and Walker, Robert L., Mathematical Methods of Physics. New York: W. A. Benjamin, Inc., 1965. P. 350.
23. Mathews, J. and Walker, R. L., *op. cit.*, p. 332.
24. Dwight, Herbert B., Tables of Integrals and Other Mathematical Data. New York: The Macmillan Company, 1961. Chapter 2, Pp. 94-101.